



# **BRNO UNIVERSITY OF TECHNOLOGY**

VYSOKÉ UČENÍ TECHNICKÉ V BRNĚ

## **FACULTY OF MECHANICAL ENGINEERING**

FAKULTA STROJNÍHO INŽENÝRSTVÍ

## **INSTITUTE OF PROCESS ENGINEERING**

ÚSTAV PROCESNÍHO INŽENÝRSTVÍ

# **FATIGUE EVALUATION METHODS FOR PRESSURE EQUIPMENT UTILISING NUMERICAL ANALYSIS RESULTS**

METODY HODNOCENÍ ÚNAVY MATERIÁLU KONSTRUKČNÍCH UZLŮ TLAKOVÝCH ZAŘÍZENÍ S VYUŽITÍM VÝSLEDKŮ NUMERICKÝCH ANALÝZ

## **MASTER'S THESIS**

DIPLOMOVÁ PRÁCE

### **AUTHOR**

AUTOR PRÁCE

**Bc. VÁCLAV BOLELOUCKÝ**

### **SUPERVISOR**

VEDOUCÍ PRÁCE

**Ing. TOMÁŠ LÉTAL, Ph.D.**

**BRNO 2020**

## Abstrakt

Diplomová práce se zabývá hodnocením únavové životnosti v okolí konstručního uzlu tlakové nádoby, kde vzniká výrazná koncentrace napětí a je zde předpoklad primárního vlivu na únavu materiálu. Konkrétně se jedná o místo přechodu kontrolního otvoru do pláště analyzovaného zařízení. Práce obsahuje teoretickou a praktickou část. V teoretické části jsou představeny pojmy a metody hodnocení, související s danou problematikou. Na základě těchto metod je provedena analýza konstrukčního uzlu tlakové nádoby. Analýza je provedena metodou konečných prvků na skořepinovém a objemovém modelu nádoby v softwaru ANSYS Workbench, její výsledky dále zpracovány a vyhodnoceny dle aktuálního návrhu úpravy evropské harmonizované normy EN 13445–3, kapitoly 18. Výsledky analýz jsou hodnoceny v závěru práce.

## Abstract

This thesis deals with the fatigue assessment of a pressure vessel structural detail. This is an area of stress concentration, thus significant influence on fatigue is expected. The thesis is divided into theoretical and practical parts. In the theoretical part, methods of the stress evaluation in the vicinity of welds are described. The subsequent finite element analysis of the inspected area based on these methods is carried out in Ansys Workbench. Final evaluation of fatigue is done according to the recent draft amendment to Clause 18 of EN 13445–3. The obtained results and methods used are discussed in the conclusion.

### Klíčová slova

Tlaková nádoba, skořepina, svarový spoj, hrdlo, extrapolace, časová životnost, MKP analýza, únava materiálu, Ansys, Solidworks, Matlab

### Keywords

Pressure vessel, shell model, welded parts, nozzle, extrapolation, fatigue life, FEA, cyclic fatigue, Ansys, Solidworks, Matlab

BOLELOUCKÝ, V. *Fatigue evaluation methods for pressure equipment utilising numerical analysis results*. Brno: Vysoké učení technické v Brně, Faculty of Mechanical Engineering, 2020. 64 s. Vedoucí Ing. Tomáš Létal, Ph.D.

# Rozšířený abstrakt

## Úvod

Hodnocení únavové životnosti tlakových nádob je většinou ukotveno v příslušných normách. Návrh tlakové nádoby, kterou se diplomová práce zabývá, spadá pod normu EN 13445-3. Podrobné hodnocení únavy je poté obsaženo v kapitole 18 této normy. Poslední vydaný návrh na úpravu kapitoly 18 si klade za cíl upravit podrobné hodnocení únavy přívětivějším směrem pro uživatele.

Předmětem diplomové práce je zhodnocení únavové životnosti v okolí místa přechodu pláště a revizního otvoru vzdušníku. Hodnocení je provedeno na základě výše zmiňovaného návrhu EN 13445-3/A20. V informativní příloze NA jsou uvedeny přístupy výpočtu napětí pomocí metody konečných prvků (MKP).

Vzdušníky jsou tlakové nádoby, sloužící k uchování stlačeného vzduchu. Můžeme je najít zejména u kompresorových stanic, kde zabraňují příliš častému spouštění kompresorů, čímž přispívají k prodloužení jejich životnosti. Technické podklady pro tvorbu modelu a následnou analýzu byly poskytnuty nejmenovanou konstrukční kanceláří.

První polovina práce je věnována únavě materiálu a metodám vyhodnocování napětí u svarových spojů. V druhé polovině práce jsou pak provedeny MKP analýzy přechodu pláště a revizního otvoru v programu Ansys Workbench.

## Popis řešení

Na základě technických podkladů byla vytvořena geometrie nádoby v programu SolidWorks. Tato geometrie byla později upravována pro potřeby MKP analýz. Analýzy byly provedeny nejdříve na skořepinovém modelu, vytvořeném ze střednicových ploch. Napětí na skořepinovém modelu bylo hodnoceno využitím lineární, respektive kvadratické extrapolace. S využitím tzv. sub-modelingu byly poté provedeny analýzy objemových modelů. Zde byla napětí získána pomocí extrapolací, linearizace napětí, Haibach-konceptu a CAB-konceptu. Pro jednotlivé metody byl pak vypočten počet dovolených cyklů.

## Shrnutí a zhodnocení výsledků

Všechny metody určování napětí se ukázaly být poměrně dobře realizovatelné a získané výsledky si poměrně dobře odpovídají. Navrhovaná úprava EN 13445-3/A20 ovšem stále vykazuje určité nejasnosti v některých částech procesu vyhodnocování napětí.

V procesu hodnocení únavy byly největší problémy zaznamenány při přípravě MKP modelů, nicméně všechny tyto problémy byly úspěšně vyřešeny. Výsledky analýz jsou přehledně uvedeny v kapitole 4.3 praktické části.

# Assignment Master's Thesis

Institut: Institute of Process Engineering  
Student: **Bc. Václav Boleloucký**  
Degree programm: Mechanical Engineering  
Branch: Process Engineering  
Supervisor: **Ing. Tomáš Létal, Ph.D.**  
Academic year: 2020/21

As provided for by the Act No. 111/98 Coll. on higher education institutions and the BUT Study and Examination Regulations, the director of the Institute hereby assigns the following topic of Master's Thesis:

## **Fatigue evaluation methods for pressure equipment utilising numerical analysis results**

### **Recommended bibliography:**

TRIEGLAFF, Ralf, Jürgen RUDOLPH, Martin BECKERT a Daniel FRIERS. Methods for Structural Stress Determination according to EN 13445-3 Annex NA – Comparison with other Codes for Unfired Pressure Vessels. MATEC Web of Conferences [online]. 2018, 165, 10003. ISSN 2261-236X. Dostupné z: doi:10.1051/matecconf/201816510003

NIEMI, Erkki a INTERNATIONAL INSTITUTE OF WELDING, ed. Stress determination for fatigue analysis of welded components. Cambridge, England: Abington Publ, 1995. ISBN 978-1-85573-213-1.

Deadline for submission Master's Thesis is given by the Schedule of the Academic year 2020/21

In Brno,

L. S.

---

prof. Ing. Petr Stehlík, CSc., dr. h. c.  
Director of the Institute

---

doc. Ing. Jaroslav Katolický, Ph.D.  
FME dean





I declare that I have written this Master's Thesis independently using exclusively the technical references and other sources of information cited in the thesis and listed in the comprehensive bibliography and that the procedure has been in accordance with Regulation S 11 of the Copyright Act No. 121/2000 Coll. of the Czech Republic, as amended.

Prohlašuji, že jsem svou práci vypracoval samostatně a použil jsem pouze podklady citované v práci a uvedené v příloženém seznamu a postup při zpracování práce je v souladu se zákonem č. 121/2000 Sb., o právu autorském, o právech souvisejících s právem autorským a o změně některých zákonů (autorský zákon) v platném znění.

Bc. Václav Boleloucký



Here I would like to acknowledge and thank my supervisor at Brno University of Technology, Ing. Tomáš Létal, Ph.D. and also my supervisor at Augsburg University of Applied Sciences, Prof. Marcus Reppich, for all their guidance and help during the work on the thesis.

Bc. Václav Boleloucký

# Contents

<b>1</b>	<b>Introduction</b>	<b>3</b>
<b>2</b>	<b>Problem Statements</b>	<b>4</b>
<b>3</b>	<b>Theoretical Background</b>	<b>5</b>
3.1	Fatigue and Fatigue Life of Welded Structures . . . . .	5
3.1.1	Stages of Crack Development . . . . .	6
3.1.2	Parameters in the Stress Cycle . . . . .	7
3.1.3	Fatigue Resistance Curves . . . . .	8
3.2	Fatigue Assessment According to EN 13445–3 . . . . .	12
3.2.1	Detailed Fatigue Life Assessment of Welded Components According to the Draft Amendment A20 . . . . .	13
3.3	Stress Raisers . . . . .	19
3.3.1	Macro–geometric Discontinuities . . . . .	19
3.3.2	Local Structural Discontinuities . . . . .	20
3.3.3	Local Notch Effect . . . . .	21
3.4	Weld Theory . . . . .	22
3.4.1	Weld Imperfections . . . . .	23
3.4.2	Weld Modelling in Shell Element Models . . . . .	24
3.5	Methods of Stress Assessment in the Vicinity of Weld Connections . . . . .	26
3.5.1	Nominal Stress Approach . . . . .	27
3.5.2	Hot–Spot Stress Approach . . . . .	28
3.5.2.1	Linear surface extrapolation . . . . .	30
3.5.2.2	Quadratic surface extrapolation . . . . .	30
3.5.2.3	Through-wall linearization . . . . .	31
3.5.2.4	CAB-concept . . . . .	32
3.5.2.5	Haibach–concept . . . . .	33
3.5.3	Effective Notch Stress Approach . . . . .	34
<b>4</b>	<b>Practical Part</b>	<b>35</b>
4.1	Vessel Geometry and Parameters . . . . .	35
4.2	Application of FEA and Fatigue Analyses . . . . .	37
4.2.1	Shell Model . . . . .	38
4.2.1.1	Geometry . . . . .	38
4.2.1.2	Mesh . . . . .	40
4.2.1.3	Boundary Conditions and Mechanical Loads . . . . .	41
4.2.1.4	FEA Associated Problems . . . . .	42
4.2.2	Solid Model . . . . .	43
4.2.2.1	Geometry . . . . .	43
4.2.2.2	Mesh . . . . .	45
4.2.2.3	Boundary Conditions and Mechanical Loads . . . . .	46
4.2.2.4	FEA Associated Problems . . . . .	47
4.3	Final Evaluation and Results . . . . .	48
<b>5</b>	<b>Conclusion</b>	<b>50</b>

<b>6 Bibliography</b>	<b>51</b>
<b>List of Abbreviations</b>	<b>54</b>
<b>List of Attachments</b>	<b>56</b>
<b>List of Figures</b>	<b>63</b>
<b>List of Tables</b>	<b>64</b>

# 1. Introduction

The presented thesis will focus on the inspection opening weld (shell/nozzle junction) fatigue assessment of an air receiver. Air receivers are usually an integral part of compressed air systems. Their purpose is mainly to store pressurized air to help compressor units deal with any pressure fluctuation that occurs in these systems.

An air receiver is a pressure vessel which undergoes cyclic loading. Therefore, fatigue may occur. For a safe operation and long lifespan of the pressure vessel, the correct fatigue life assessment is crucial. Close surroundings of welded parts are one of the most decisive areas in regards to fatigue. This is because of stress concentrations caused by discontinuities (such as holes or weld imperfections) and geometrical complexities that are present in these areas. The inspection opening of the vessel investigated in this thesis is a case of such critical area. Determining the acting stresses is further influenced by the presence of other factors such as tension arising during cooling of the weld with insufficient after-treatment, when the tension in the material stays uneven. In practice, finite element analysis (FEA) is the preferred method used in certain steps of the fatigue assessment of welded structures. If the setting of the calculation model is done correctly, the results from FEA can be very accurate.

In this diploma thesis, the fatigue assessment of the shell/nozzle junction will be evaluated on two FEA models. The first model will be a shell model of the examined pressure vessel represented by mid-surfaces. The second model will be made from solid bodies with a thickness which corresponds to the real pressure vessel. General stress assessment methods and guidance for the evaluation of fatigue will be described in the first part of this thesis. The shell/nozzle junction will be evaluated in the second part of the thesis according to methods recommended in the draft amendment EN 13445-3/A20 [10]. This will include surface extrapolation, stress linearization, Haibach-concept, and CAB-concept.

## 2. Problem Statements

The fatigue life assessment procedure consists of several main steps. At first, the geometry which includes welds in the evaluated area has to be precisely modeled. Here, any overlaps of adjacent bodies are restricted to prevent problems in the pre-processing phase. The geometry is based on drawings provided by a selected design engineering office. In the next step, the reference points and paths for the finite element analysis have to be determined. Then, a suitable mesh has to be prepared to ensure good time to accuracy ratio of the analyses. Lastly, the fatigue life will be calculated based on stresses acting along the reference paths according to EN 13445-3/A20 [10].



# 3. Theoretical Background

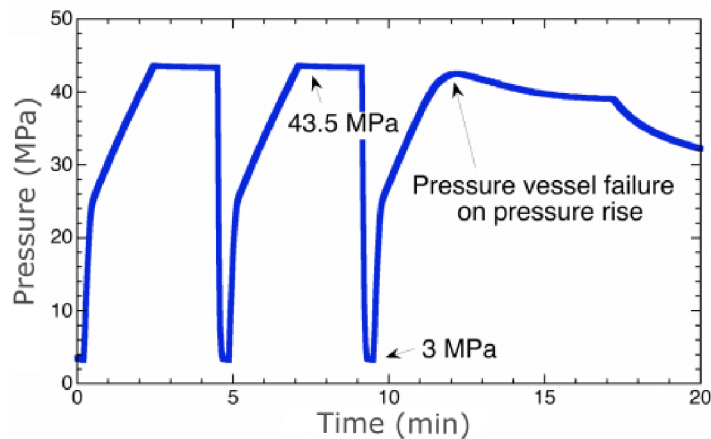
This chapter summarizes basic knowledge relevant for this diploma thesis. At first some basics of the fatigue process will be introduced. This will include stages of fatigue life, stress cycles, fatigue resistance curves and fatigue life assessment procedure of welded structures. The second half of the theoretical part will present geometrical factors influencing the stress values, basics to theory of welds, recommendations on weld modeling and stress assessment methods in vicinity of weld connections.

## 3.1. Fatigue and Fatigue Life of Welded Structures

Damage inside structures exposed to repeated loading is known as fatigue. In structures loaded by fluctuating forces (e.g. snow, wind, pressure, temperature changes) a permanent deformation or a crack can occur even when the yielding point of the material across the cross-section has not been reached. This phenomenon occurs as a result of damage accumulation through the entire loading history.

Tiny material imperfections can never be avoided. These imperfections can grow in size and can subsequently cause fatigue failure when exposed to a sufficiently large value of fluctuating stress. Therefore for design engineers, it is crucial to be able to determine the resulting impact of the repeated loading on the structure. This means assessing the total life cycles to crack initiation that may lead to the component's failure. This is referred to as fatigue life.[1, 2]

Decisive factors for the assessment of the component's fatigue life are: acting stress range, stress raisers (notches, discontinuities, etc.) and elastic behaviour of the material.



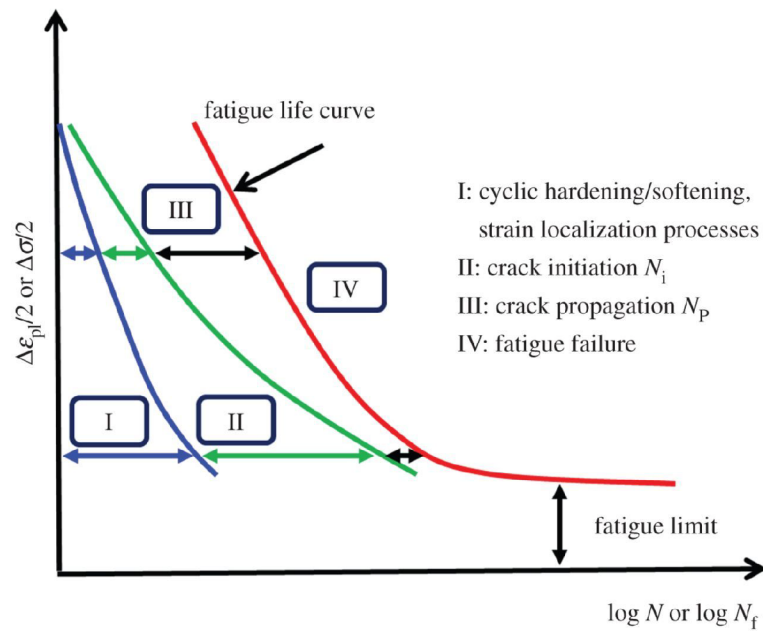
**Figure 3.1:** Pressure cycles right before the fatigue failure [6]

Figure 3.1 represents an example of a fatigue failure of a pressure vessel filled with gaseous hydrogen. Common pressure cycles are ranging between 3 and 43.5 MPa. In the last peak, the critical number of 8 048 life cycles had been reached which resulted in a sufficient crack growth that caused the pressurized gas to escape to the surroundings.

### 3.1.1. Stages of Crack Development

The stages in the process of fatigue have no strict boundaries and one stage can partially overlap with another. In general, the fatigue process can be divided into four phases as follows: [1]

- Strain localization processes (leading to transcrystalline fractures on the surface)
- Crack initiation (usually propagates from the surface)
- Crack growth (stable or unstable)
- Ultimate ductile failure.



**Figure 3.2:** Representation of the four fatigue phases in ductile metals before failure [4]

As stated earlier in the text, small imperfections in the material are always present to a certain degree. This is especially true in the case of welded structures since they all have microfractures stemming directly from fabrication. This makes the crack initialization phase more unpredictable. Hence, it can be assumed that the initial stage of crack development has already been reached. With this assumption, only the two last stages of the fatigue process are relevant for the evaluation. However, this fact has already been included during the creation the fatigue curves for welded materials described in 3.1.3. [3] During fatigue failure, the bonds between atoms break perpendicularly to the applied tensile stress which allows the crack to further propagate until the final rupture.

In regards to the number of life cycles and applied loading: a large stress amplitude which overlaps with the yield strength causes the material to plasticize significantly and leads to the so-called low cycle fatigue which is characterized by a fatigue life up to  $10^4$  cycles. When fatigue life exceeds this number, it begins to be called high cycle fatigue which is generally associated with the stress amplitude cycling purely in the elastic zone. [1]

### 3.1.2. Parameters in the Stress Cycle

Figure 3.3 shows a general loading cycle with a sinusoidal character. In practice, the real cycles often have variable amplitude and the stress characteristic in time is rarely ideal. This can result in a relatively complicated mathematical description. To make the computational formulae easier the cycles are replaced by mathematically simpler functions which have the same impact on fatigue life of the structure as the original cycle.

The stress fluctuation presented below (loading with a constant amplitude) is typical for the air receiver which is the subject of this thesis. However, in the case of welded components a variable loading amplitude is more common. [15]

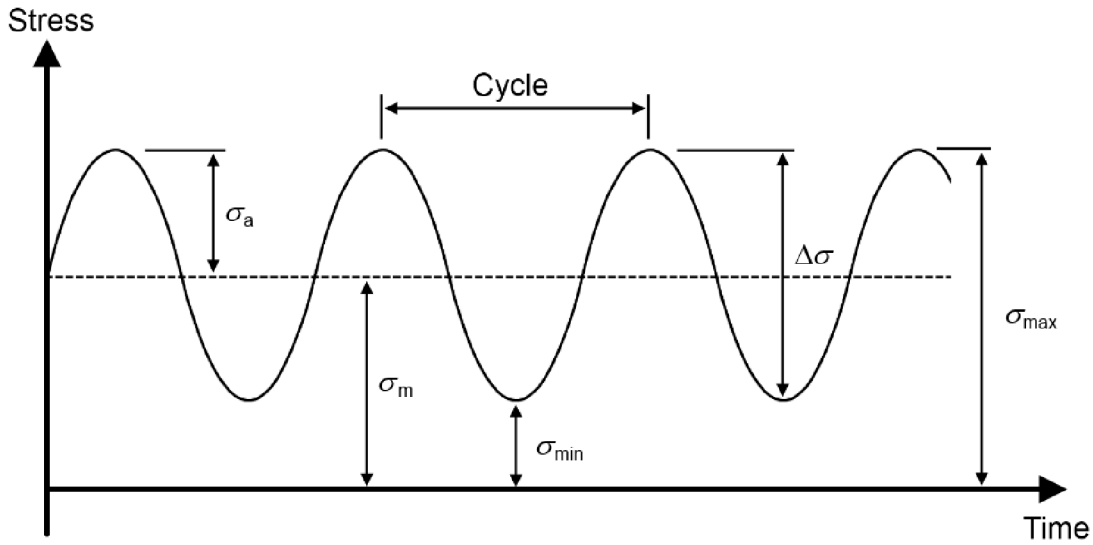


**Figure 3.3:** Stress cycle parameters [18]

$\sigma_a$  – stress amplitude;  $\sigma_m$  – mean stress of the cycle;

$\sigma_{max}$  – maximal applied stress;  $\sigma_{min}$  – minimal applied stress;  $\Delta\sigma$  – stress range

The following equations apply to the basic stress cycle characteristics: [17]

$$\sigma_m = \frac{\sigma_{max} + \sigma_{min}}{2} \quad (3.1)$$

$$\sigma_a = \frac{\sigma_{max} - \sigma_{min}}{2} \quad (3.2)$$

The main parameter of fatigue life assessment is the stress range:

$$\Delta\sigma = \sigma_{max} - \sigma_{min} = 2\sigma_a \quad (3.3)$$

The stress ratio (R-ratio) is also an important factor for the description of the stress cycle: [19, 17]

$$R = \frac{\sigma_{min}}{\sigma_{max}} \quad (3.4)$$

### 3.1.3. Fatigue Resistance Curves

Material resistance to fatigue is, in many cases, derived from tensile stress tests with a constant or variable amplitudes.<sup>1</sup> The data obtained from these tests are plotted to a graph using logarithmic coordinates. They are referred to as S–N (stress–number) curves (sometimes also called Wöhler curves). The x–axis shows the number of cycles to failure and y–axis shows the stress amplitude. Typical shape of an S–N curve for an unnotched low–alloy steel is shown in figure 3.4 below.<sup>2</sup>

The curve starts at the ultimate tensile strength point and continues to descend linearly through the low cycle fatigue and high cycle fatigue zones. This linear behaviour can be described by the Basquin equation.<sup>3</sup> Around approximately  $10^6$  cycles, the fatigue limit value  $S_f$  is achieved (= endurance limit stress, for steel alloys usually about 35–50 % of the material ultimate tensile strength).

With an amplitude below that limit, the specimen can withstand a theoretically infinite number of loading cycles (the tests are usually performed for a maximum number of  $10^7$  repetitions). This means that the stress amplitude will no longer cause any crack growth and the fatigue failure will not be a limiting criterion for the component’s operating life. However, this does not mean that the fatigue limit is also a threshold for crack initiation in general. [2, 7]

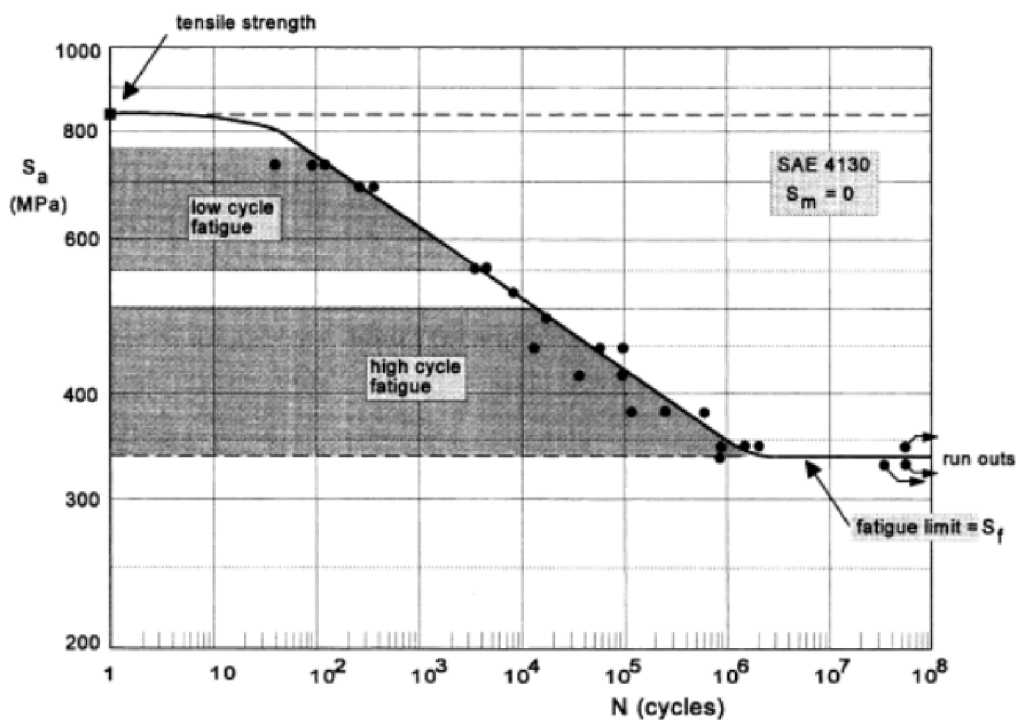


Figure 3.4: S–N curve for unnotched low–alloy steel specimens [7]

<sup>1</sup>More regarding the testing procedure can be found in [7]

<sup>2</sup> $S_a = \Delta\sigma = 2\sigma_a$

<sup>3</sup>Basquin equation:[5]  $N_f = N_0 \left(\frac{S}{S_0}\right)^{\frac{1}{b}}$ , where  $N_f$  = number of cycles to failure;  $N_0, S_0$  = points on the material curve;  $b$  = slope of the material curve

### 3.1. FATIGUE AND FATIGUE LIFE OF WELDED STRUCTURES

In the assessment of the welded component's fatigue resistance the fatigue strength of the parent material must also be taken into account.

S-N curves for welded components and various other structural details are classified into so-called FAT classes (see fig. 3.5). These take the form FATxxx, where FAT stands for fatigue class and xxx represents the value of the fatigue resistance of the particular structural detail or weld in *MPa* at  $2 \cdot 10^6$  cycles. The assessment of the fatigue resistance for welds and other details is mostly based on the nominal value of the maximum range of the principal stress, which acts on the section most susceptible to a potential rupture. However, S-N curves and their classification can also be found for the assessment of loaded details on their own. Both of these cases are based on the maximum value of the stress range in a critical spot of the detail. [2]

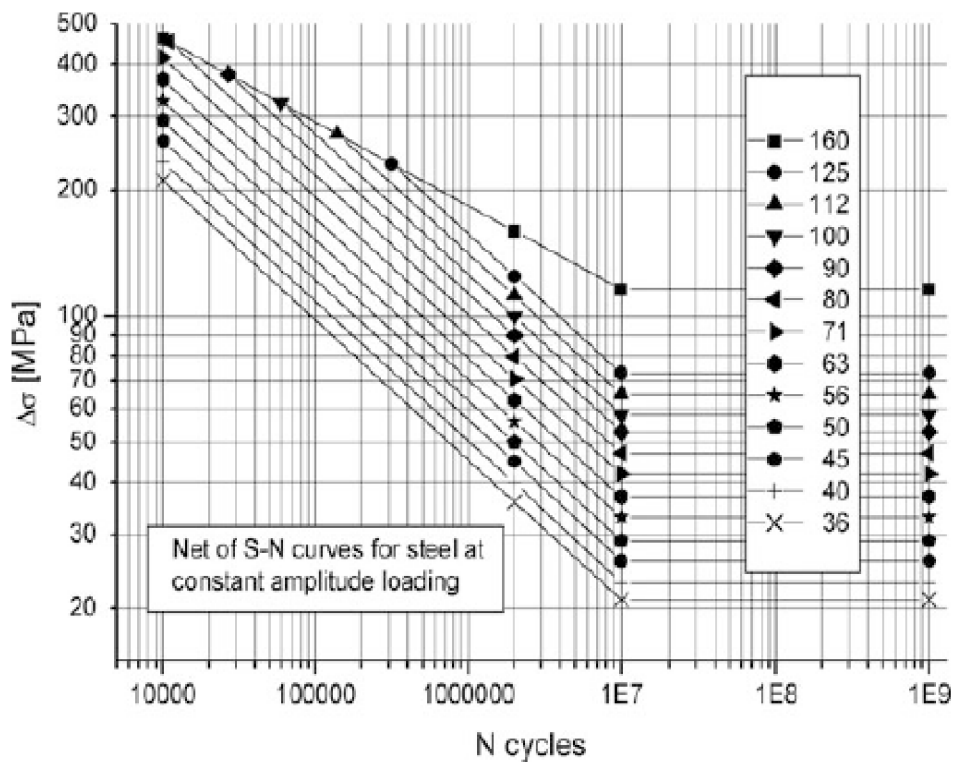


**Figure 3.5:** S-N curves for steel categorized in FAT classes; standard application [2]

The curves in the graph (3.5) are expressed mathematically as follows:

$$N = \frac{C}{\Delta\sigma^m} \text{ or } N = \frac{C}{\Delta\tau^m} \quad (3.5)$$

where the exponent  $m$  represents the slope of the curve and  $C$  represents the empirical constant. For the S-N curves in Fig. 3.5, based on normal stresses, the slope is  $m = 3$  and it is assumed that the amplitude fatigue limit correlates with  $10^7$  cycles. In the case of S-N curves based on shear stresses, the slope of the curve is  $m = 5$  and the amplitude fatigue limit corresponds to  $10^8$  cycles. [2]



### 3. THEORETICAL BACKGROUND

During the fatigue life prediction, one should be aware of the fact that S–N curves for very high cycle applications behave slightly differently under the fatigue limit (see Fig. 3.4 below). The infinite life line no longer exists in the horizontal direction but instead shows a slight slope. The S–N curve continues to decline from that point on with approximately 10 % in stress per decade in cycles. Such decline corresponds to  $m = 22$ . However, this is applicable to very high cycle operations only and is still subject to extensive research.[2]

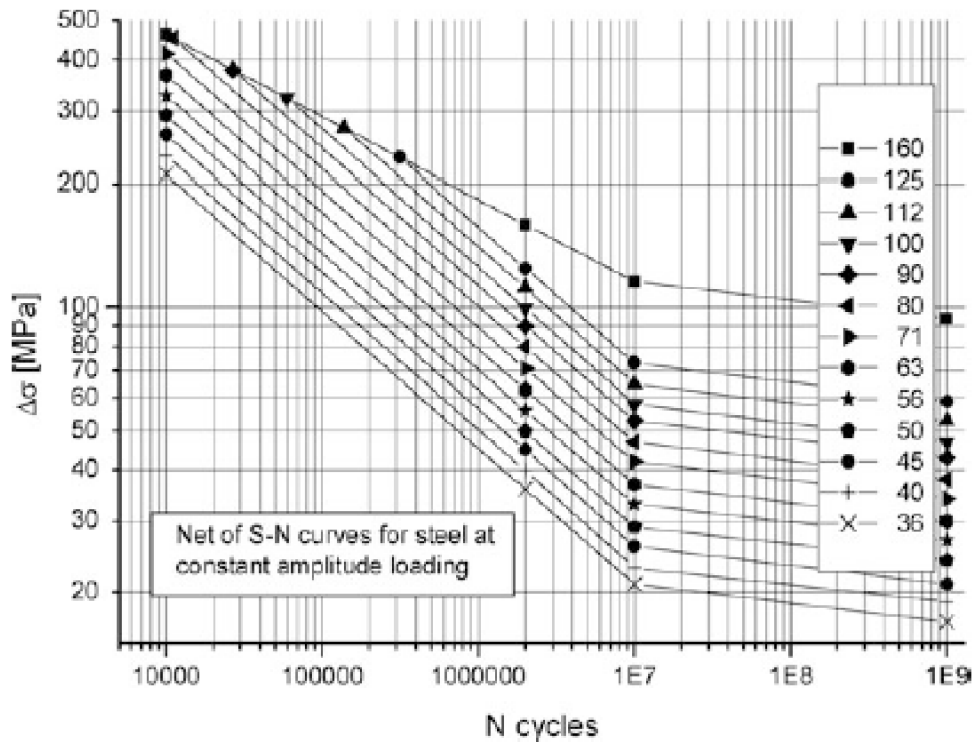


**Figure 3.6:** S–N curves for steel categorized in FAT classes, very high cycles applications [2]

*“The fatigue curves are based on representative experimental investigations and thus include the effects of:*

- *structural hot spot stress concentrations due to the detail shown*
- *local stress concentrations due to the weld geometry*
- *weld imperfections consistent with normal fabrication standards*
- *direction of loading*
- *high residual stresses*
- *metallurgical conditions*
- *welding process (fusion welding, unless otherwise stated)*
- *inspection procedure (NDT), if specified*
- *post weld treatment, if specified” [2]*

### 3.1. *FATIGUE AND FATIGUE LIFE OF WELDED STRUCTURES*

Regardless of everything that fatigue curves for the structural details include, the information such as quality, shape and size of the weld are taken into account only partially. This means that the information conform to a standard quality based on common welding methods and are described in codes and standards. In the case of lower or higher qualities a fatigue test should be performed to verify suitability of the welding conditions. [2]

In case of fracture mechanics approach, the fatigue strength data are given as a stress intensity factor range  $\Delta K$  versus a crack growth rate ( $da/dN$ ). The fatigue crack propagation rate data is obtained from fatigue tests where the crack propagation is measured. [2]

## 3.2. Fatigue Assessment According to EN 13445–3

Two fatigue assessment approaches can be found in Clauses 17 and 18 of the third part of the European Pressure Vessel Standard EN 13445. While Clause 17 focuses on a simplified fatigue life assessment method, Clause 18 represents a method of a detailed fatigue life assessment. In this thesis, only the more complex approach based on the Clause 18 *"Detailed assessment of fatigue life"* will be used in the fatigue life evaluation. The evaluation is performed on the inspection opening of the vessel.

Based on recommendations made by the International Institute of Welding (IIW), Clause 18 has been recently newly revised, consolidated and now is in the inquiry phase (see [10]). In addition, new informative annexes NA – ND have been introduced in the document. The aim of the proposed modifications is to make the guidelines for the application clearer and more user-friendly.

According to [8], there are six major points in the newly revised document to be emphasized:

- Detailed instructions for fatigue assessment of welded components established on structural stress and structural hot-spot stress approach
- Detailed instructions for determining relevant stresses and stress ranges have been given based on the type of the FEA models (brick and shell type)
- Detailed instructions for the proper counting of loading cycles
- Critical plane approach implementation [8]
- Techniques for the improvement of welds
- In-service monitoring criteria

In the case of unwelded components the rules remain unchanged. But the rules have changed for welded components. For them, parts 18.6 *"Stresses for fatigue assessment of welded components and regions"* and 18.10 *"Fatigue strength of welded components"* are used. [11] In the first case, adjustments of the determination method of relevant stress ranges have been made. Part 18.10 deals with revisions of fatigue curves and other relevant weld details.

As the fatigue assessment is, according to the Clause 18, usually made using FEA, the newly introduced annex NA *"Examples of determination of the structural hot-spot stress by finite element analysis using shell or solid elements"* gives detailed guidelines in this field.

The new informative annex NB *"Cycle Counting and determination of equivalent stress range"* deals with the cycle counting problem and the determination of the equivalent stress ranges for checking fatigue. Implementation of the critical plane approach is also part of the annex.

Guidelines for partially penetrated welds which are modeled by solid elements can be found in the new informative annex NC *"Fatigue assessment of partial penetration welds"*. The new informative annex ND *"Table of stress concentration factors  $K_t$ "* provides a table of stress concentration factors for various applications.[8, 9]



### 3.2.1. Detailed Fatigue Life Assessment of Welded Components According to the Draft Amendment A20

In this section, the detailed evaluation method of fatigue life according to the newly revised Clause 18 and the new informative annex NA will be introduced with particular emphasis on welded components. Please keep in mind that this amendment is distributed for reviews and comments only and has not been integrated into EN 13445 yet. [10]

A schematic representation of the main steps in the detailed fatigue life assessment is given in the block diagram below (Fig. 3.7). As already mentioned above, Clauses 18.6 and 18.10 are the most relevant ones for welded components. The other parts of Clause 18 which are shown in the diagram apply to both welded and non-welded components.

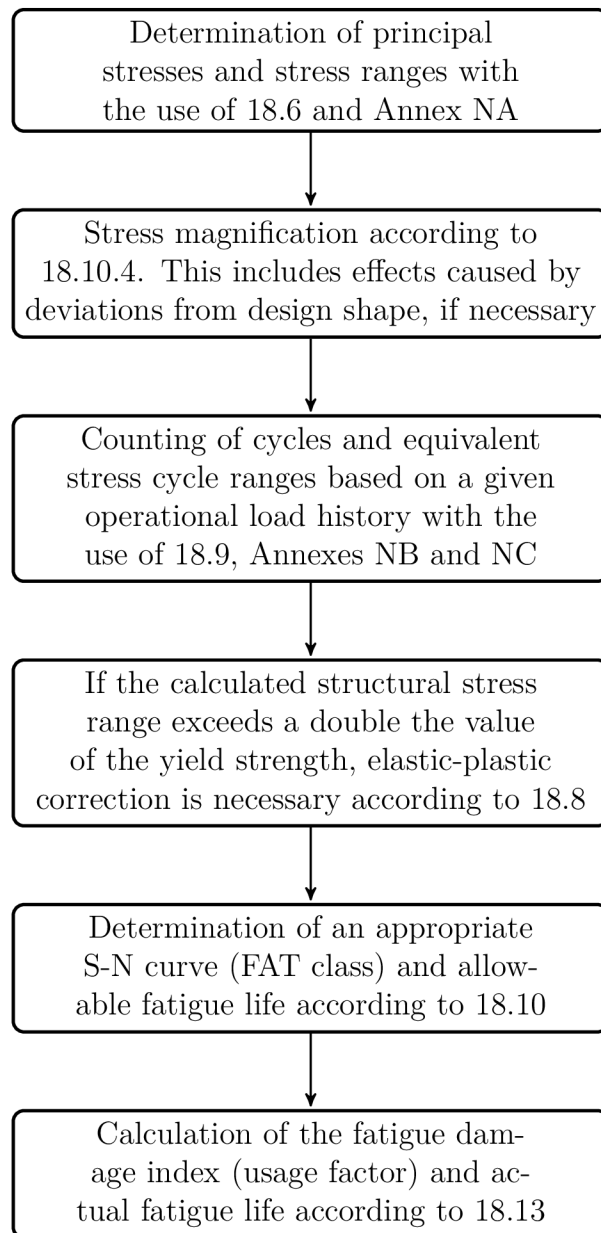


**Figure 3.7:** Fatigue assessment of welded components – detailed procedure [10]

### 3. THEORETICAL BACKGROUND

As the first step, it is necessary to evaluate acting stress ranges. This should be performed with the help of Clause 18.6 "Determination of stresses for fatigue assessment of welded components and zones" [11]

Generally, the examined stresses in the fatigue life assessment are dependent on the weld type: [10]

- In the case of aligned seam welds and simple attachments that are not placed in regions affected by gross structural discontinuities, the calculated nominal stress is based either on a formula or FEA.
- In the case of partial penetration welds, according to Annex NC, and double-sided fillet welds used for connecting attachments that are loaded externally, the average stresses across the weld throat should be used for the assessment.
- In the case of full penetration welds and similar welds, structural stresses at the point where a crack initiation can occur (so-called hot-spot) should be used for the fatigue assessment. This also includes reinforcing plate welds which are placed around branches and nozzles.
- In the case of the possible combination of mechanical stresses and thermal loads generating highly nonlinear stresses, the stress can be determined on the basis of FEA with solid elements while utilising surface extrapolation, CAB or Haibach methods.

A calculation of the structural hot-spot stress can be carried out based on one of the following approaches described in 18.6 and more thoroughly detailed in Annex NA:[10]

- *Linear surface extrapolation (hot-spot stress)*

Where the through cross-section stress distribution in the hot-spot is approximately linear (membrane plus bending as is the case in thin shells), stresses can be determined with the use of linear extrapolation according to Annex NA. Stress values are examined on the surface at the specified distances  $l_1 = 0.4e$  and  $l_1 + l_2 = 1.0e$  from the hot-spot (where  $e$  means thickness of the base material) and subsequently extrapolated to the hot spot.

- *Quadratic surface extrapolation (hot-spot stress)*

Where the through cross-section stress distribution is nonlinear (e.g. may result from thick sections, local forces, etc.), stresses can be determined using a quadratic extrapolation according to Annex NA. Stress values are examined on the surface at the specified distances  $l_1 = 0.5e$ ,  $l_1 + l_2 = 1.5e$  and  $l_1 + l_2 + l_3 = 2.5e$  from the hot-spot and subsequently extrapolated towards it.

- *Through-wall linearization*

This approach linearizes the stresses through the section thickness to the hot-spot (see Annex NA) using path linearization in solid type finite element model. [9]

### 3.2. FATIGUE ASSESSMENT ACCORDING TO EN 13445-3

- *CAB-concept*

This approach removes the stress singularity in a solid finite element model by rounding the weld with an appropriate radius (CAB method) according to Annex NA.

- *Haibach-concept*

This method is based on the use of the stress at a position 2.5 mm in front of the weld toe based on Haibach (see Annex NA).

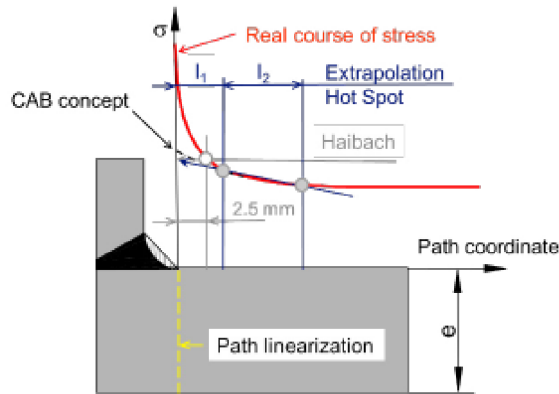


**Figure 3.8:** Structural stress determination methods according to Annex NA [8]

In the second step of a welded component fatigue life assessment, any deviations from the design shape should be incorporated into the calculation of stresses. These deviations from the intended shape can take the form of various discontinuities and misalignments, as shown in Fig. 3.9, where local increase in stress is generated and thus a lowered resistance to fatigue is expected. [8]

*”Departures from intended shape include misalignment of abutting plates, an angle between abutting plates, roof-topping where there is a flat at the end of each plate, weld peaking and ovality. In most cases these features cause local increases in the hoop stress in the shell but deviations from design shape associated with circumferential seams cause increases in the longitudinal stress.”* [10]

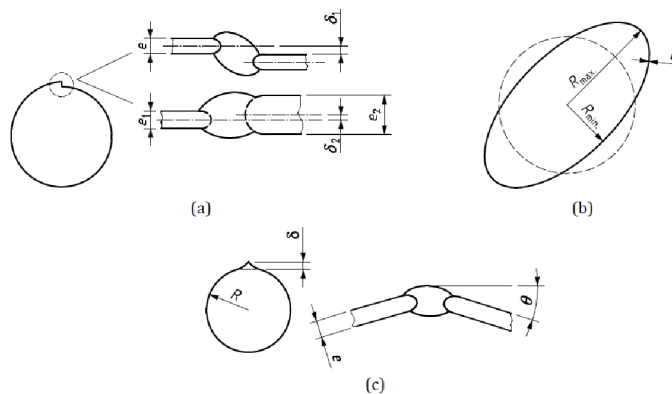


**Figure 3.9:** Representation of deviations from design shape at the seam welds, taken from [10]

### 3. THEORETICAL BACKGROUND

The increase of stresses can be determined either by including these misalignments into the geometry of the finite element model or by applying appropriate corrections; this is applied when the stress evaluation of the nominal geometry is used. [8]

The next phase of the assessment would normally be the cycle counting procedure. This applies to the cases of variable amplitude fluctuation or when more cycle amplitudes occur during each one loading event. For the purposes of this thesis, the stress fluctuation is considered to be constant. Here, the cycle counting procedure is unnecessary.

The counting of cycles can be done with the use of the Clause 18.9 and Annexes NB and NC. These Annexes present a detailed guidance on how to determine stress cycles from a given operational load history or specified design load.

When stress ranges, evaluated as critical, exceed double the value of the yield strength, it is necessary to apply elastic-plastic correction according to 18.8. The correction factor in the case of mechanical loading is given as follows: [10]

$$k_e = 1 + A_0 \left( \frac{\Delta\sigma_{eq,l}}{2R_{p0,2/T^*}} - 1 \right) \quad (3.6)$$

where

- for ferritic steels with  $800 \leq R_m \leq 1000 \text{ MPa}$

$$A_0 = 0.5$$

- for ferritic steels with  $R_m \leq 500 \text{ MPa}$  and for all austenitic steels

$$A_0 = 0.4$$

- for ferritic steels with  $800 \leq R_m \leq 1000 \text{ MPa}$

$$A_0 = 0.4 + \frac{(R_m - 500)}{3000}$$

The corrected stress range for welded joints is then  $\Delta\sigma_{eq} = k_e \cdot \Delta\sigma_{eq,l}$

For purely thermally induced stresses, the correction factor  $k_v$  is also given in [10]. For stress evaluated in the vicinity of local discontinuities where a detailed analysis is not made, the correction factor  $k_e$  should be used for thermal loadings instead of  $k_v$ . The correction factor  $k_e$  must also be used in cases of combined thermal and mechanical loading. [10]

With the knowledge of the actual stress range the fatigue life determination can be approached according to 18.10. Firstly, the class of the weld detail must be determined. This is done using the table 18-4. It should be noted that, for a single joint type, the weld class can differ depending on the testing group. Details which do not conform to examples given in the table 18-4 should be considered as class 32 unless the resistance is proven either by special fatigue tests or by a reference to relevant test results. [10]

### 3.2. FATIGUE ASSESSMENT ACCORDING TO EN 13445-3

In 18.10, a few correction factors can be found which are important for the final fatigue life assessment. These are determined by the following terms: [10]

- **Thickness correction factor**  $f_{ew}$ <sup>4</sup>

- for material thickness  $e_n > 25 \text{ mm}$

$$f_{ew} = \left( \frac{25}{e_n} \right)^{0.25} \quad (3.7)$$

- for  $e_n \leq 25 \text{ mm}$

$$f_{ew} = 1$$

- for  $e_n > 150 \text{ mm}$

$$f_{ew} = 0.6389$$

- **Temperature correction factor**  $f_{T^*}$ ,

where

$$T^* = 0.75 \cdot T_{max} + 0,25 \cdot T_{min} \quad (3.8)$$

- for ferritic materials and mean cycle temperatures  $T^* > 100 \text{ }^\circ\text{C}$

$$f_{T^*} = 1.03 - 1.5 \cdot 10^{-4}T^* - 1.5 \cdot 10^{-6}T^{*2} \quad (3.9)$$

- for austenitic materials and mean cycle temperatures  $T^* > 100 \text{ }^\circ\text{C}$

$$f_{T^*} = 1.043 - 4.3 \cdot 10^{-4}T^* \quad (3.10)$$

- for mean cycle temperatures  $T^* < 100 \text{ }^\circ\text{C}$

$$f_{T^*} = 1$$

- *Mean stress correction factor for fully stress-relieved welded components*  $f_{m^*}$

- for testing groups 1 or 2 and fully penetrated welds

$$f_{m^*} = \max \left( 1; 1.3^{\frac{0.4343 \cdot \ln N - 4.699}{1.602}} \cdot f_m \right) \quad (3.11)$$

where  $f_m$  is the correction factor for unwelded components given in 18.11.13.1

- for testing group 3 and partially heat treated welds

$$f_{m^*} = 1$$

- **Combined correction factor**

$$f_w = f_{ew^*} \cdot f_{T^*} \cdot f_{m^*} \quad (3.12)$$

---

<sup>4</sup> $f_{ew} = 1$  when the Haibach method is used

### 3. THEORETICAL BACKGROUND

Finally, the number of fatigue life cycles is determined by using the appropriate S–N curves for the weld detail chosen in table 18–4 in [10].

The S–N curves take the form of:

$$N = \frac{C}{\Delta\sigma_R^m} \quad (3.13)$$

In this equation,  $\Delta\sigma_R$  is the specified stress range,  $N$  stands for the permissible number of stress cycles and  $C$  and  $m$  are coefficients of S–N curves. More information related to S–N curves can be found in Chapter 3.1.3.

- if  $\frac{\Delta\sigma_R}{f_w} \geq \Delta\sigma_D$

$$N = \frac{C_1}{\left(\frac{\Delta\sigma_R}{f_w}\right)^{m_1}} \quad (3.14)$$

– where  $C_1$  and  $m_1$  are coefficients of S–N curves for  $N \leq 5 \cdot 10^6$  cycles

- if  $\Delta\sigma_{Cut} \leq \frac{\Delta\sigma_R}{f_w} < \Delta\sigma_D$

$$N = \frac{C_2}{\left(\frac{\Delta\sigma_R}{f_w}\right)^{m_2}} \quad (3.15)$$

– where  $C_2$  and  $m_2$  are coefficients of S–N curves for  $N > 5 \cdot 10^6$  cycles

– when all stress ranges are smaller than the endurance limit  $\Delta\sigma_D$ , the allowable number of stress cycles  $N$  is considered to be infinite

- if  $\frac{\Delta\sigma_R}{f_w} < \Delta\sigma_{Cut}$ ,  $N = \text{infinity}$

Values of the  $C_1$  and  $C_2$  coefficients, the cut-off limit  $\Delta\sigma_{Cut}$  and the endurance limit  $\Delta\sigma_D$  can be taken from table 18–7 in [10] or calculated by the following formulae:

$$C_1 = (class)^3 \cdot 2 \cdot 10^6 \quad C_2 = (class)^5 \left(\frac{2}{5}\right)^{\frac{5}{3}} \cdot 5 \cdot 10^6 \quad (3.16)$$

$$\Delta\sigma_D = (class) \left(\frac{2}{5}\right)^{\frac{1}{3}} \quad (3.17)$$

$$\Delta\sigma_{Cut} = (class) \left(\frac{2}{5}\right)^{\frac{1}{3}} \cdot (5 \cdot 10^{-2})^{\frac{1}{5}} \quad (3.18)$$

Welding flaws in fatigue loaded vessels can be tolerated to some extent. According to 18.13.5 planar flaws are unacceptable. For "fatigue design-critical areas", tolerance levels of embedded non-planar and geometric flaws are given in EN 13445-5:2014, Annex G (standard for non-cyclic operation). "Fatigue design-critical areas" are such areas where the value of the designed cumulative fatigue damage index  $D_{f\text{design}}$  is greater than 0.5. [10]

The value of the cumulative fatigue damage  $D_f$  cannot be greater than 1 and is calculated as follows: [10]

$$D_f = \frac{n_1}{N_1} + \frac{n_2}{N_2} + \dots = \sum \frac{n_i}{N_i} \quad (3.19)$$

where  $n$  is the specified number and  $N$  is the allowable number of cycles.



### 3.3. Stress Raisers

In actual products, geometrical discontinuities (such as holes, welds, curves, etc.) are always present to a certain level which can eventually lead to locally increased stress values. These stress peaks can then have a major influence on the service life of cyclic-loaded structures. These phenomena, which cause the rise of stress values, will be presented in this chapter with a particular focus on welded components.

#### 3.3.1. Macro-geometric Discontinuities

Macro-geometric discontinuities, also called gross structural discontinuities, affect the distribution of strain and stress across the entire thickness of a wall over a significantly large region. [11] These discontinuities can be located, for example, in the areas of head to shell/nozzle to shell junctions, large openings in general, and other types shown in Figure 3.10.

Welded structures often contain macro-geometrical elements and shapes which are not included in the classified details given in the design codes. Examples of these forms are shown in Fig. 3.10 below. For some of these forms, analytical formulae can be found in technical literature which, if combined with basic stress analysis methods, give useful results for the overall stress distribution throughout the structure. [15]

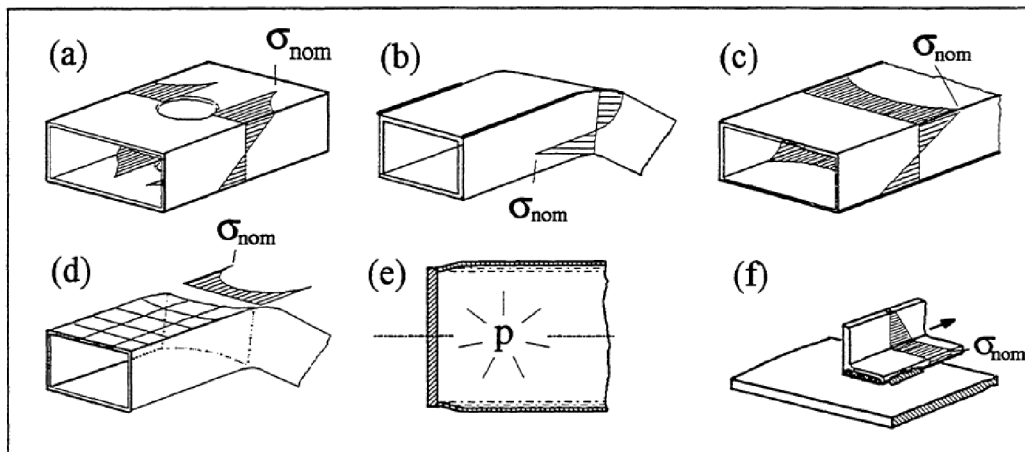


**Figure 3.10:** Common types of macro-geometric effects where: a) large openings; b) curved beam; c) shear lag; d) flange curling; e) discontinuity stresses in a shell; f) bending due to lap joint eccentricity [2]

Stresses caused by these stress raisers must be taken into account in all types of stresses, especially when the fatigue analysis is based on nominal stresses. This is because these macro-geometric effects are not included in fatigue resistance based on simple test specimens. However, in the case of geometries for which S-N fatigue curves have already been determined this rule does not apply.[15]

### 3.3.2. Local Structural Discontinuities

Structural discontinuities shown in Fig. 3.11 affect the stress and strain distribution locally and not across the entire cross section (in comparison with the macro-geometric discontinuities). Such local discontinuities are usually already included in fatigue tests for welded structures.[15]

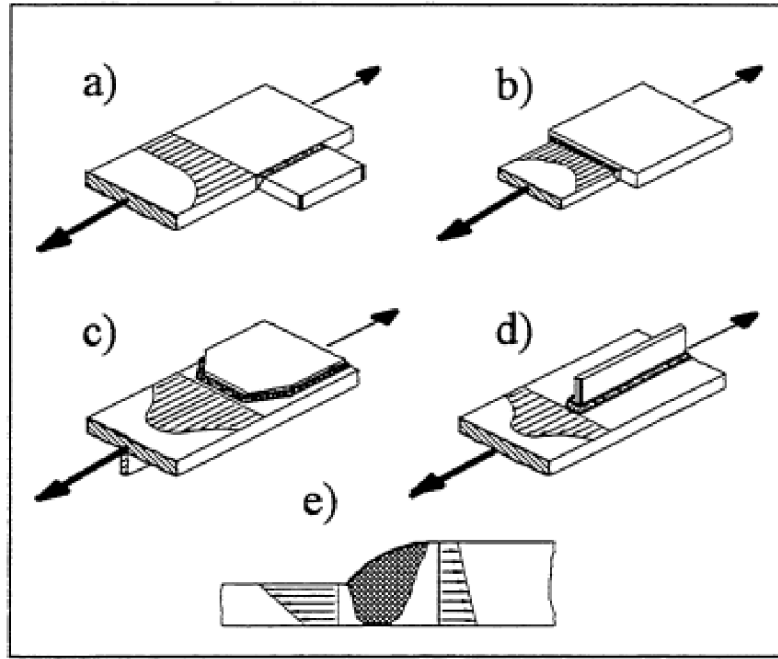


**Figure 3.11:** Local structural discontinuities: (a) gusset plate; (b) variation in width; (c) cover plate end; (d) stiffener end; (e) variation in plate thickness. [15]

Extra membrane and shell bending stresses caused by structural discontinuities do not belong to the nominal stress category and should be considered as a part of structural stress category instead.

Unfortunately, pure analytical approaches generally cannot be used to analyse stress and deformation effects of structural discontinuities of components. Therefore, the evaluation of deformation and stress caused by local discontinuities is usually supported by the use of FEA. But such analyses are often relatively expensive and require a lot of experience in this field to be effective. This is why suitable parametric formulae, which would relate hot-spot stress and geometry, are needed. This could be done using FEA or direct strain measurements. In literature, only a few structural details (e.g. tubular joints) regarding this problem have been covered so far. [15]



### 3.3. STRESS RAISERS

#### 3.3.3. Local Notch Effect

Welded parts often have bead roughness (or blow holes) in the weld which locally cause increased stress (act as local notches). This is why the local notch effects occur in welded components with substantial frequency. Local notches have no impact on the structural stress (= shell and bending stresses). However in terms of the fatigue life assessment, their effect on the structure is very significant. [15]

Figure 3.12 shows a nonlinear behaviour in stress distribution caused by the notch effect. The nonlinearity practically vanishes approximately  $0.4t$  from the weld toe and the behaviour in the stress distribution can be again considered as linear.[12] The nonlinear stress peak is located near the surface. Therefore, defects occurring on the surface tend to be more critical than defects under the surface, where the stress value is significantly lower. [15]

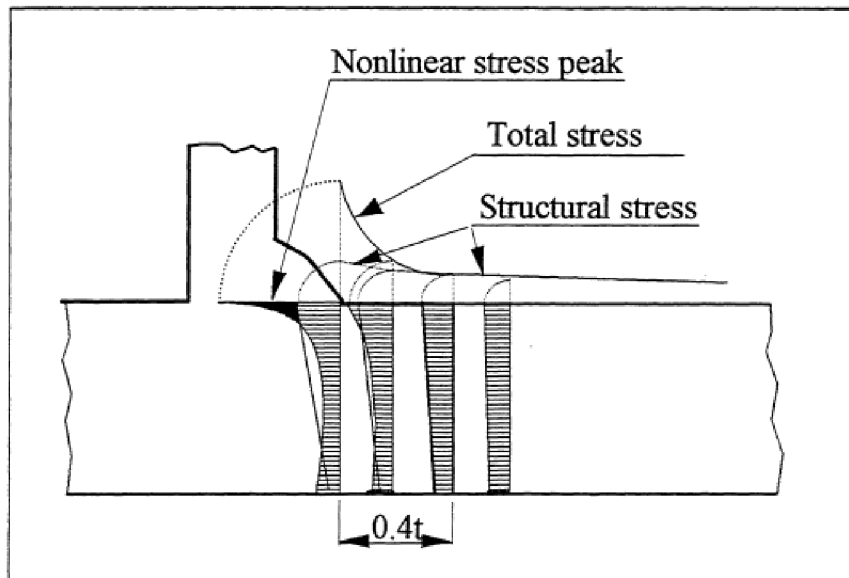


**Figure 3.12:** Local stress distribution in vicinity of a weld toe [15]

The notch stress can be calculated by multiplying the structural (hot-spot) stress by a stress concentration factor. When more precise results are needed, the stresses can be multiplied by a theoretical notch factor,  $K_t$ , or determined using FEA. In this case, the mesh in an area near the weld should be relatively fine because of a very steep stress gradient in the notch. This would otherwise lead to highly inaccurate results. Subsequently, stress calculated based on elastic assumptions exceeds the material's yield strength in many cases. Therefore, the calculated stress should be considered a pseudo-elastic stress. [15]

Since the effect of the nonlinear stress peak is implicitly incorporated in fatigue test results (and thus in S-N curves), it does not need to be calculated when nominal or hot-spot methods are used for the fatigue analysis. [15]

### 3.4. Weld Theory

Welding is the main part of the pressure vessel manufacturing process. Most welded joints spend a significant portion of their service life in the crack propagation phase which makes them highly susceptible to fatigue failure. [20]

The reason for that are stress concentration effects in the vicinity of discontinuities of the weld geometry (see Chapter 3.3). These are the side effects of the welding process. Figure 3.13 shows an increase of stress cycle amplitude at the weld toe.

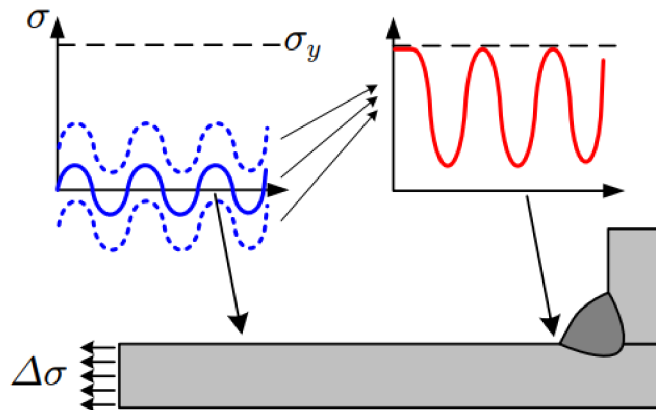


**Figure 3.13:** Increase of a stress cycle amplitude at the weld toe [20]

For joining two or more parts different weld types are used. The most common ones are the butt and fillet welds. Figure 3.14 shows a fillet weld with possible modes of failure. The butt weld cracking behaves similarly, thus, the following figure can also be applied to this type of weld.

For better monitoring and detection purposes during the component's service life, fatigue cracking which starts from the weld toe is generally more advantageous than cracking which starts from the root of the weld. Nevertheless, toe and root cracking are critical for the weld fatigue assessment and the calculated component must be designed with all three of the modes in mind.[22]

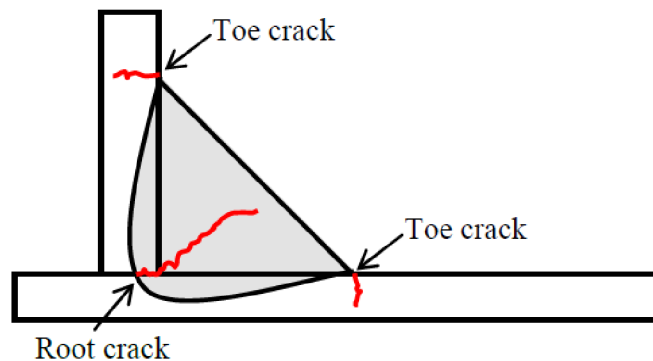


**Figure 3.14:** Modes of fatigue failure of a fillet weld [22]

### 3.4. WELD THEORY

Since the welds should be easy to model in FEA, the fillet weld geometry is sometimes considered to be triangular in simulations to make the modeling process easier for the designer. In another illustration of the fillet weld in 3.15,  $a$  is the thickness of the weld throat (height of the assumed triangle) including the weld penetration, whereas  $a_0$  is the nominal dimension of the throat thickness and is hence the value prescribed in drawings.[22]

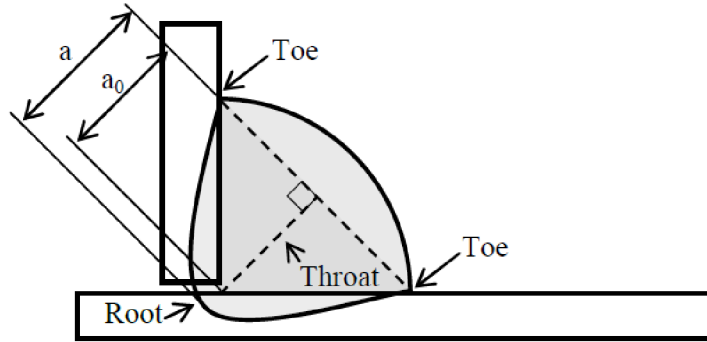
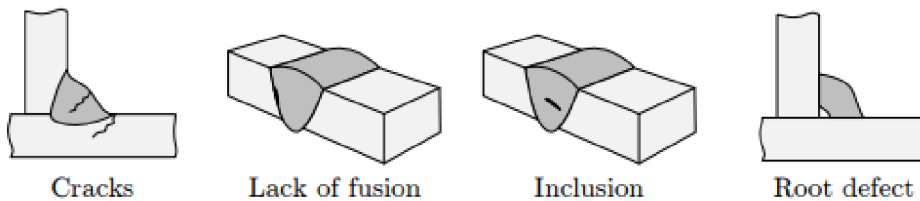


Figure 3.15: Fillet weld parameters [22]

#### 3.4.1. Weld Imperfections

According to the generally accepted standard for quality of welds according to ISO 5817 there are "26 different types of weld imperfections, as e.g. cracks, porosity, worm holes, inclusions, lack of penetration, lack of fusion, lack of fit, undercut, excessive weld overfill, insufficient weld throat, root overfill, misalignment, weld sag, incomplete root, cold lap, arc strike, sputter etc. For each of these imperfections, the allowable extent of each type of imperfections is tabulated for the different quality levels B, C and D." [14] In most standards and codes a standard level of weld quality with regards to ISO 5817 is specified. Also, additional regulations must be provided.[14]

(a) Not allowed:



(b) Main requirements:

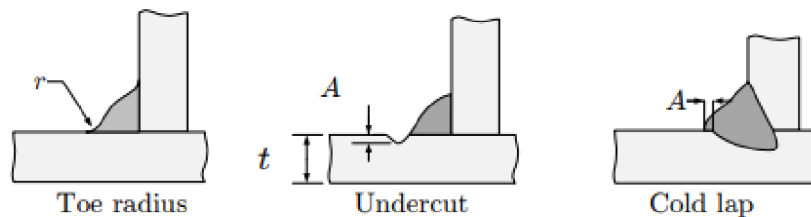


Figure 3.16: Typical weld imperfections [20]

The quality levels are based on various tolerances to weld imperfections. Some examples of defects which can occur during welding are shown in Fig. 3.16. Cracks and other significant imperfections, where the risk of early fatigue cracking may be higher, are not allowed. On the other hand, some defects such as transitions which are not perfectly smooth, undercuts or cold laps may be tolerated to some extent, if the given requirements are met. According to the recommendations of IIW the welds yielding to fatigue phenomenon should always be classified as quality level B. The selection of weld qualities is also included in the European standard Eurocode 3 as well as in EN 13445-4 and depends on the quality of the material used, production and consequences.[20, 2]

When the weld quality seems to be insufficient, the fatigue resistance can be improved by so-called post-weld treatments (PWT). These include several methods such as shape and geometry improvements or residual stress condition improvement.[14, 20] In Figure 3.17 two main types of improvements of welded joints are illustrated. In (b) the weld toe radius is smoothed out and the notch effect becomes less significant. Residual stress improvement shown in (c) causes the mean stress value to move towards zero which results in less extreme stress values during the loading cycle.

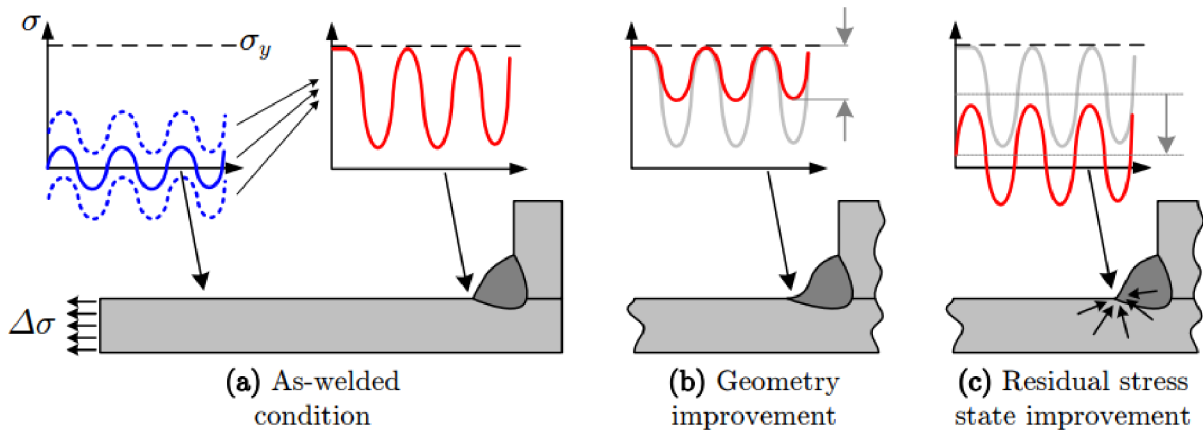


Figure 3.17: Examples of stress improvement methods [20]

### 3.4.2. Weld Modelling in Shell Element Models

There are several methods and recommendations for weld modeling. Generally, to be able to evaluate the effective notch stress a complete weld geometry must be considered in the FE model. In the case of hot-spot stress determination using simple shell elements, there is no need to incorporate the weld in the model. However, in cases where it is hard to distinguish the nonlinear notch effects in stress distribution from effects caused by geometrical discontinuities or in cases of significant influence from bending stresses, the weld should be already included in the model. [16]

Welds can be easily included in the model when solid-element FE models are used. On the other hand, when the model is created using shell elements, the weld modeling becomes more complicated for the designer. Therefore, several simplified methods were developed by taking the modeling effort and the influence of the weld stiffness into account.

### 3.4. WELD THEORY

The results obtained may vary depending on the particular method. Choosing the right method requires great experiences in modeling.

Figure 3.18 represents frequently used techniques for weld modeling which use shell elements. In the model S1, inclined elements are used, but only inside the area of the actual fillet weld. Connection to the plates is then done via rigid links. This approach offers a good stiffness incorporation all the while the cross-sectional area in the model more or less corresponds to the actual area. [12] Model S2 replaces the weld connection between plates by an inclined rigid link. This method is relatively feasible, though the actual weld cross-sectional area is not incorporated. For the S2 model, linear elements are recommended. In the case of the S3 model no weld is modeled at all. The connection is done via shell elements of the plates. Here the weld stiffness can be incorporated to some extent by increasing the thickness in the area of the connection. In the S4 model, the link is realized using inclined elements with a single mid-side node. The length of the link is recommended to be equal to two weld thicknesses (3.4). [12, 16]

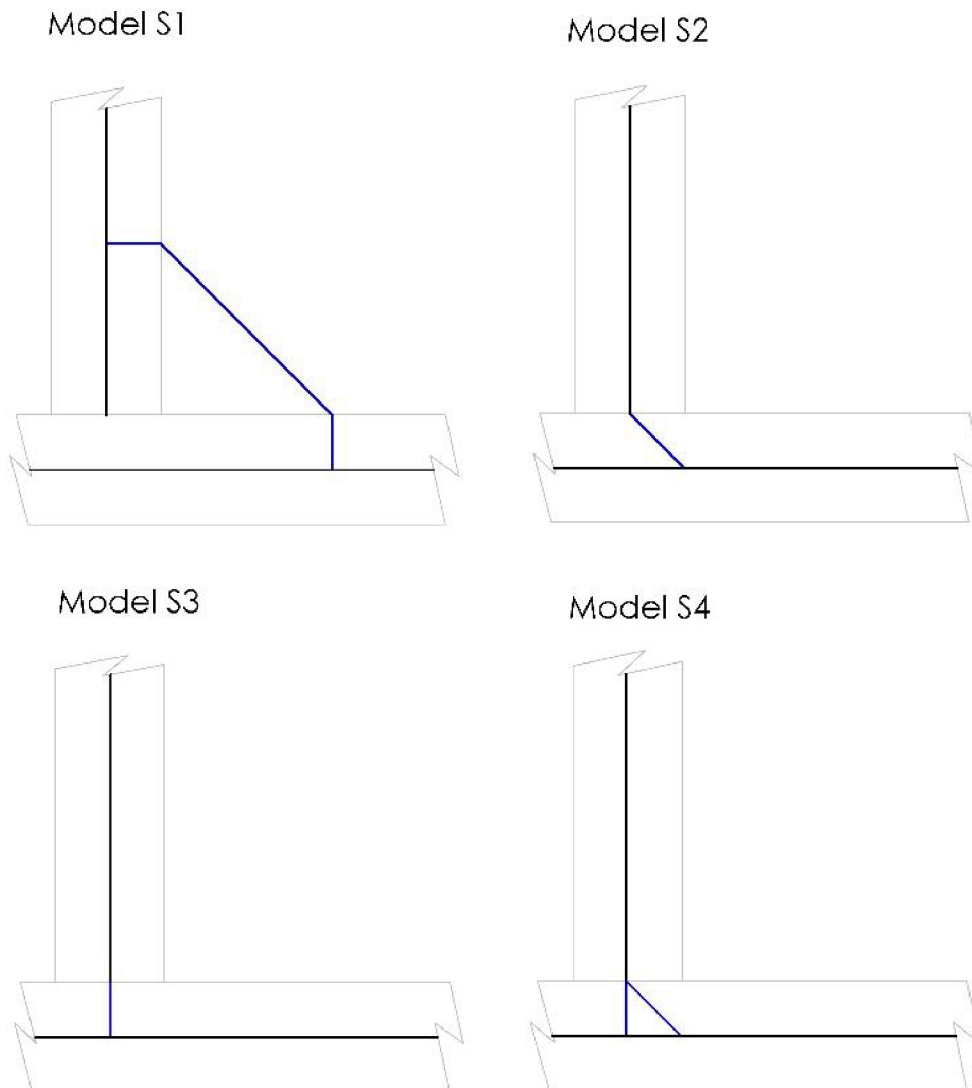


**Figure 3.18:** Examples of weld modelling techniques using shell elements [21]

### 3.5. Methods of Stress Assessment in the Vicinity of Weld Connections

This chapter will explain the four stress assessment methods mentioned in Chapter 3.2.1. All these approaches can be divided into groups according to Table 3.1 below. The most common and also the simplest approach is the nominal stress method which does not take any local stress raisers into account. In welded structures, it is typically the local geometry of the weld. Other approaches already include discontinuities caused by welds. However, the hot-spot stress approach disregards notch areas with very local stress concentration caused by the radius of the weld bead. This effect is taken into account when approaches such as notch stress or fracture mechanics are used.[13, 16]

In the first three methods mentioned above, which consider the linear elastic theory or FEA, the subsequent assessment of fatigue life is done by the evaluation of S-N curves (3.1.3). The fourth approach mentioned is based on the principles of fracture mechanics. [16] Fatigue life estimation which uses this approach is independent of all S-N curves. For the purposes of this thesis, only the first three approaches will be described in detail.

**Table 3.1:** Stress evaluation methods for welded structures (table taken entirely from [2])

Type	Stress raisers	Stress determined	Assessment procedure
A	None	Gross average stress from sectional forces, calculated using general theories, e.g. beam theory	Not applicable for fatigue analysis of joints, only for component testing
B	Macro-geometrical effects due to the design of the component, but excluding stress concentrations due to the welded joint itself.	Range of the nominal stress (also modified or local nominal stress)	Nominal stress approach
C	B + structural discontinuities due to the structural detail of the welded joint, but excluding the notch effect of the weld toe transition	Range of the structural hot-spot stress	Structural hot-spot stress approach
D	A + B + C + notch stress concentration due to weld bead notches (a) actual notch stress (b) effective notch stress	Range of the elastic notch stress (total stress)	(a) fracture mechanics approach (b) Effective notch stress approach



### 3.5. METHODS OF STRESS ASSESSMENT IN THE VICINITY OF WELD CONNECTIONS

Methods further described in the text are graphically represented in Figure 3.19. Stress distribution through the plate's thickness changes as the stress rises in the direction towards the weld. Applying forces to the component causes stresses in the material. The parent material contributes to the strength of the welded structure but only up to a certain distance from the weld. Within this area, the stress field is influenced by bending moments and shear forces which change towards the weld. If there are no other discontinuities in the structure, the stress value outside of this area which is influenced by the weld remains constant across the thickness.

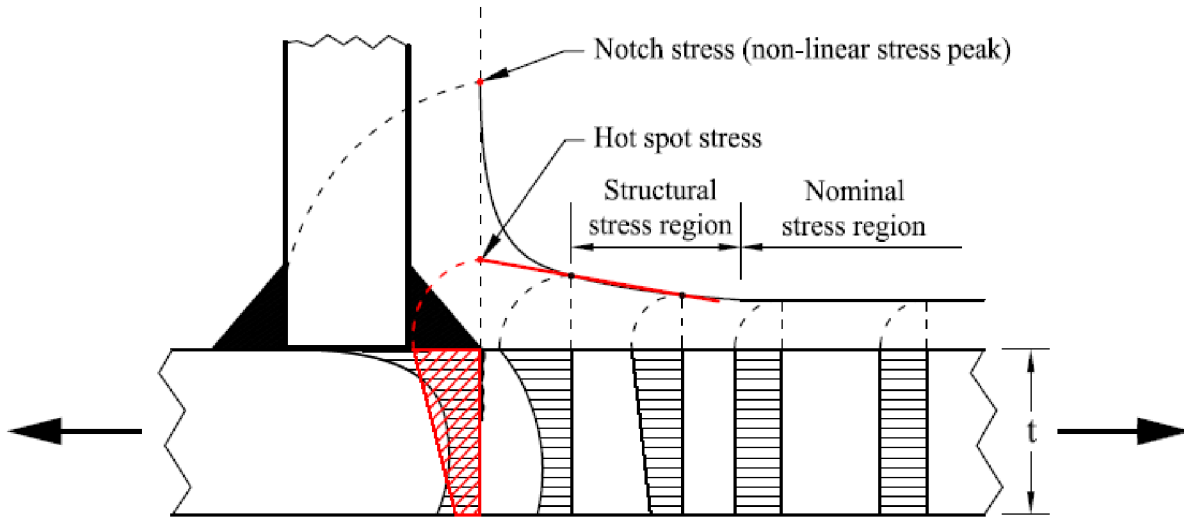


Figure 3.19: Graphical representation of stress evaluation methods [16]

#### 3.5.1. Nominal Stress Approach

The nominal stress approach considers the stress values in the weld to be the same as the ones in areas not influenced by the weld. Linear elastic behaviour of the material is considered. If the evaluated geometry is simple enough (e.g. cylindrical shells, beams, etc.) the nominal stress can be relatively easily calculated using analytical methods, conforming to the assumptions given above. Another field where the use of nominal approach would be appropriate are cases for which other methods such as the hot-spot or the notch stress methods do not work well, e.g. for longitudinally loaded welds. [3, 2] However, the effects caused by the macro-geometric discontinuities must be taken into account when performing calculations. The effect of the construction geometry on stress distribution is described in 3.3.1. [2]

Since the method is relatively easy, it is covered by many standards and recommendations. FAT classes, which already include effects of notches, are available for fatigue assessment of various geometries. However in the case of too complex geometry, FAT classes are not available and the nominal stress approach does not work well anymore. Instead, another fatigue life assessment method should be considered. [12, 2]

### 3.5.2. Hot-Spot Stress Approach

The Hot-Spot stress approach has been developed for cases where the evaluation that is based on the nominal stress is too complicated due to loading and geometric complexities. With the development of FEA, this approach is becoming more important as well as more widely used. [16]

The term "hot-spot stress" refers to a critical point of structural stress (membrane + shell bending stress) in a structure. It is usually located at the weld toe where notches and discontinuities are located. [15]

The hot-spot (structural) stress approach covers all stress concentration effects of the inspected detail, except for the nonlinear stress peak effects which are caused by the weld itself (see Fig. 3.19). The models for FEA are considered to be ideally welded for this. The reason for neglecting the notch effect in the approach is that the designer is usually unable to know the actual geometry of the weld in advance. Implicitly, the S-N curves which are experimentally determined for various FAT classes consider the influence of notches. Examples of structural discontinuities along with their distribution of structural stresses are represented in Figure 3.11. [2, 12]

In general, the hot-spot stress can be obtained by measurements or calculations which use FEA. In this case, the nonlinear stress peak is eliminated either by stress linearization across the thickness of the plate or by extrapolation methods. Here, depending on the method, two or three reference points are specified on the surface of the plate in given distances from the weld toe. At these reference points, which are defined by stress evaluation paths perpendicular to the weld axis (as shown in Figure 3.20), stress values are determined and subsequently linearly or quadratically extrapolated to the weld toe. The first reference point from the weld toe has to be outside of the zone that is influenced by the notch, as described in the introduction to this chapter. The commonly used "safe" distance is  $0.4t$  where  $t$  represents thickness of the plate. In the recent draft amendment to the Clause 18 (see [10]), however, the closest reference point is specified at the distance  $0.5t$  from the weld toe. This is for the purposes of quadratic surface extrapolation. [2, 14]

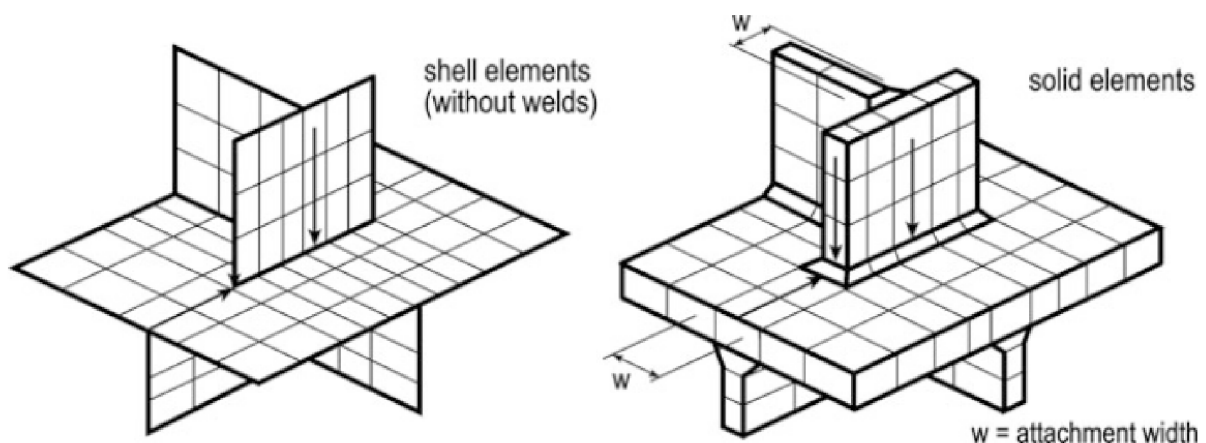


**Figure 3.20:** Typical hot-spot stress evaluation paths used for FEA (stress along the edge does not depend on the material thickness, stress along the surface depends on the material thickness) [2]



### 3.5. METHODS OF STRESS ASSESSMENT IN THE VICINITY OF WELD CONNECTIONS

As already mentioned earlier, FEA is an appropriate tool for hot-spot stress evaluation. FEA is also helpful when there is a need for parametric formulae for diverse structural details.

Since only local yielding occurs, purely elastic behavior of the material is assumed in the analysis. Elements used in computational models for the analysis can be either shell or solid types. Because the hot-spot is commonly found in regions with high stress gradients, results may differ significantly depending on the used element type and sizing. This leads, together with high mesh sensitivity, to more time expensive model creation. Therefore, to obtain relevant results of the structural detail stresses it is important to follow certain rules (e.g. lengths of elements should be determined by the distance of reference points where the first nodal point should be closest to the hot-spot in order to avoid singularities).[12]

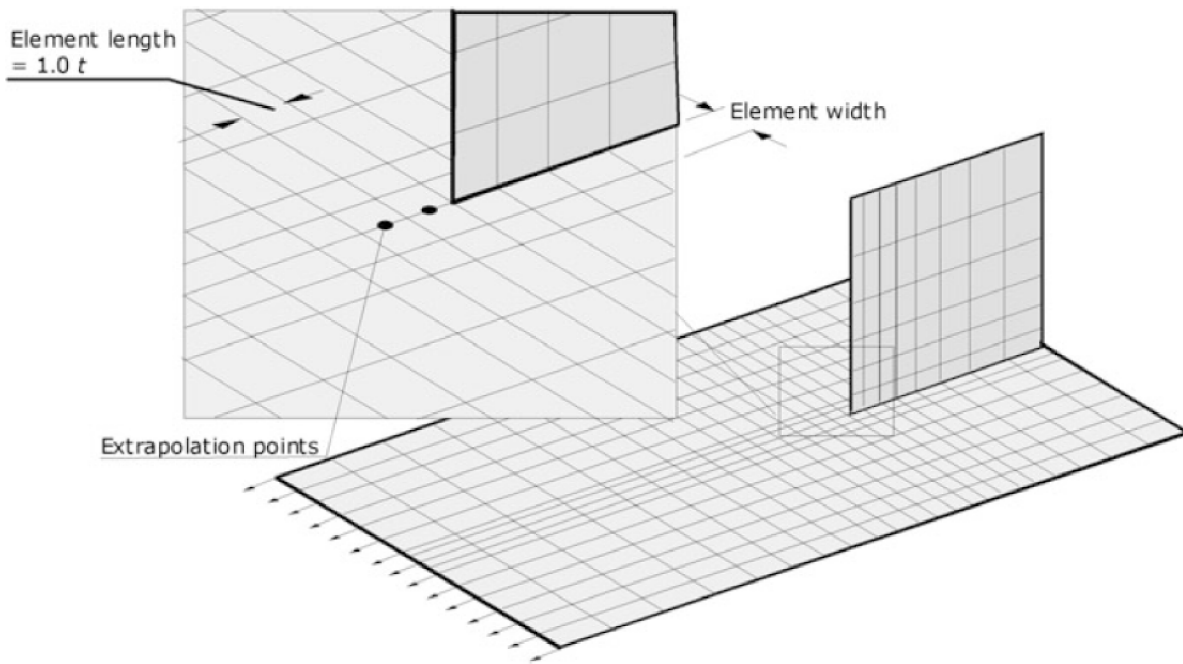


**Figure 3.21:** Location of reference points at a shell model with a relatively coarse mesh [12]

Thoroughly described procedures of hot-spot stress determination including reference points and elements are given in the recommendations by the IIW. European standard for unfired pressure vessels EN 13445-3, however, gives no explicit recommendations regarding this. In the draft amendment of newly revised Clause 18 [10] of the aforementioned standard some general rules and guidances are included. For further information and alternative approaches it refers to the IIW recommendations. Another limitation of the hot-spot stress method for fatigue assessment is that only cracking which starts from the weld toe is considered here. Currently, the IIW gives no recommendations on how to use the extrapolated structural stress for the assessment of joints where the cracking starts from the weld root. [13]

Hot-spot determination approaches according to the draft amendment newly revised Clause 18 are listed in the following subsections: [10]

### 3.5.2.1. Linear surface extrapolation

Two reference points are specified each at a distance given by the terms  $L_1 = 0.4 \cdot t$  and  $L_1 + L_2 = 1.0 \cdot t$  respectively. Linear surface extrapolation to the hot-spot is shown in Figure 3.22. In the shell model on the left,  $B$  represents the extrapolated hot-spot, 1 represents the real structure and 2 represents the shell element. Apparent difference between these two cases is that if the model consists of shell elements and at the same time the weld is not included the distance should be measured from the intersection point in order to avoid possible non-conservative results. In the case of the solid model the distance is measured from the weld toe. [10] However, it is possible to extrapolate to the intersection when the position of the weld toe cannot be known before the manufacturing phase. In the recommendations from IIW the guideline goes further and specifies different distances of the reference points needed for evaluating the hot-spot based on its location on the plate and on mesh sizing. [2, 12]

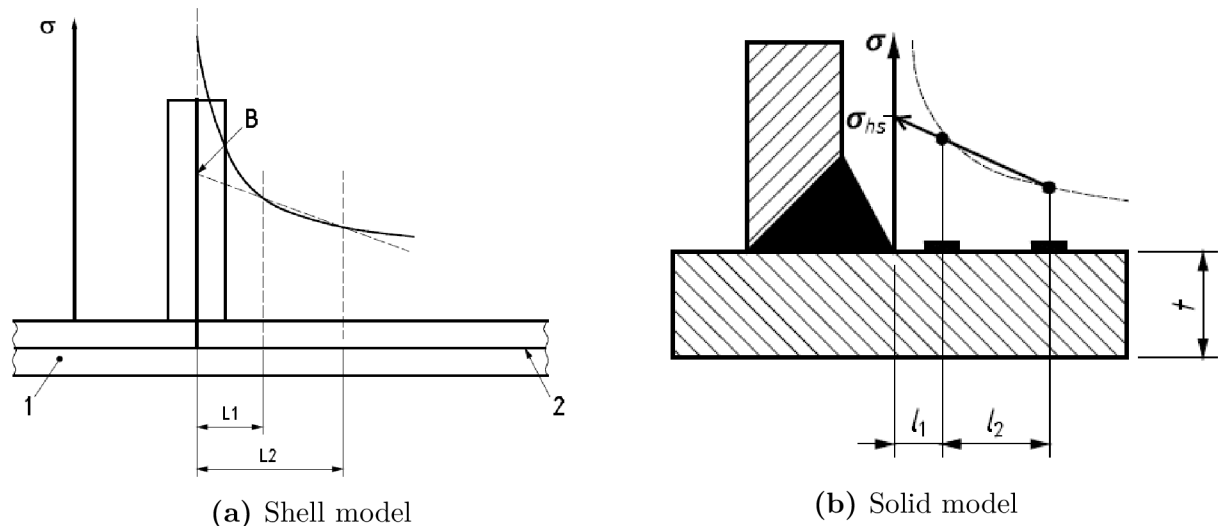


Figure 3.22: Linear extrapolation based on two specified reference points [10]

### 3.5.2.2. Quadratic surface extrapolation

The quadratic extrapolation in Figure 3.23 is a very convenient method for cases of a significantly nonlinear behaviour in the stress field in the direction to the hot-spot, for thick-walled structures or for cases where the direction of the applied force rapidly changes. [2] Two reference points are specified at distances given by the terms  $L_1 = 0.5 \cdot t$ ,  $L_1 + L_2 = 1.5 \cdot t$  and  $L_1 + L_2 + L_3 = 2.5 \cdot t$ . [10].

For quadratic surface extrapolation, the recommended distances of the reference points according to IIW differ from the way the distances are specified in the draft amendment of Clause 18 [10]. The distances are:  $0.4 \cdot t$  for the closest point,  $0.9 \cdot t$  for the second point, and  $1.4 \cdot t$  for the third point. [2] This also applies to the case when the weld toe is located on a plate surface. [12]

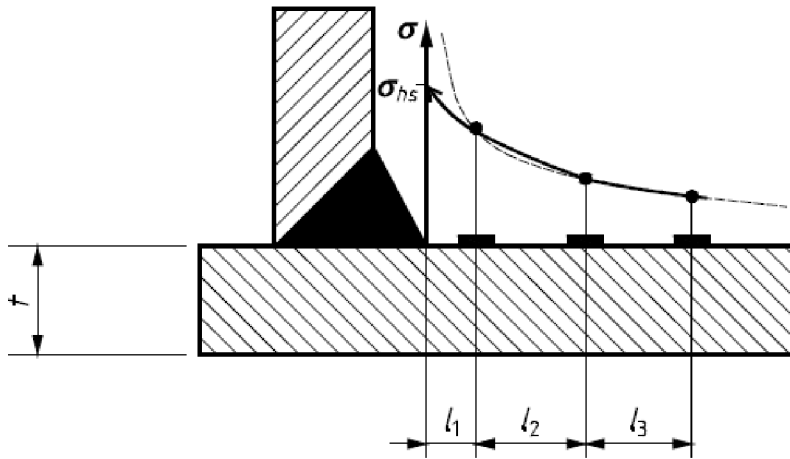


Figure 3.23: Quadratic extrapolation based on three reference points [10]

### 3.5.2.3. Through-wall linearization

Figure 3.24 shows a graphical representation of the through-wall linearization method. The stress distribution is linearized through the entire cross section of the plate at the position of the weld toe. For the evaluation of hot-spot stress, a sum of the linearized bending stress plus the membrane stress is used. [10]

Through-wall linearization *”is particularly useful for cases where the structural stress distribution in front of the weld toe is nonlinear and for relatively thick structural components. In the latter, location of the read-out points for surface stress extrapolation far away from the weld toe may cause certain geometric effects on the local stress to be missed.”* [12] This method is generally applicable only to hot-spots where the weld toe lies on the surface of the plate and not at the edge of the plate (see Fig 3.20). [2]

Another limitation can be seen, for instance, at the ends of the attachment when shell elements are used. The result can then be exaggerated because of the stress singularity compared to a case when solid elements are used. For these cases, surface stress extrapolation is the preferred method. [12] Detailed guidelines for the through-wall linearization method can be found in [23, 12].

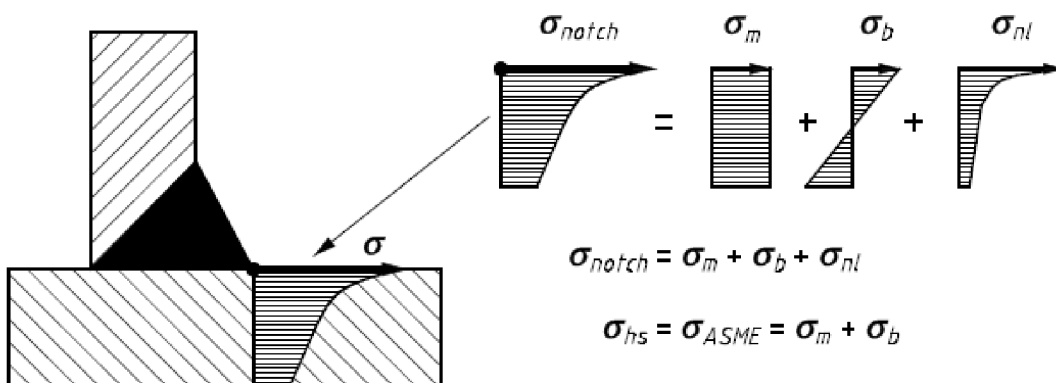
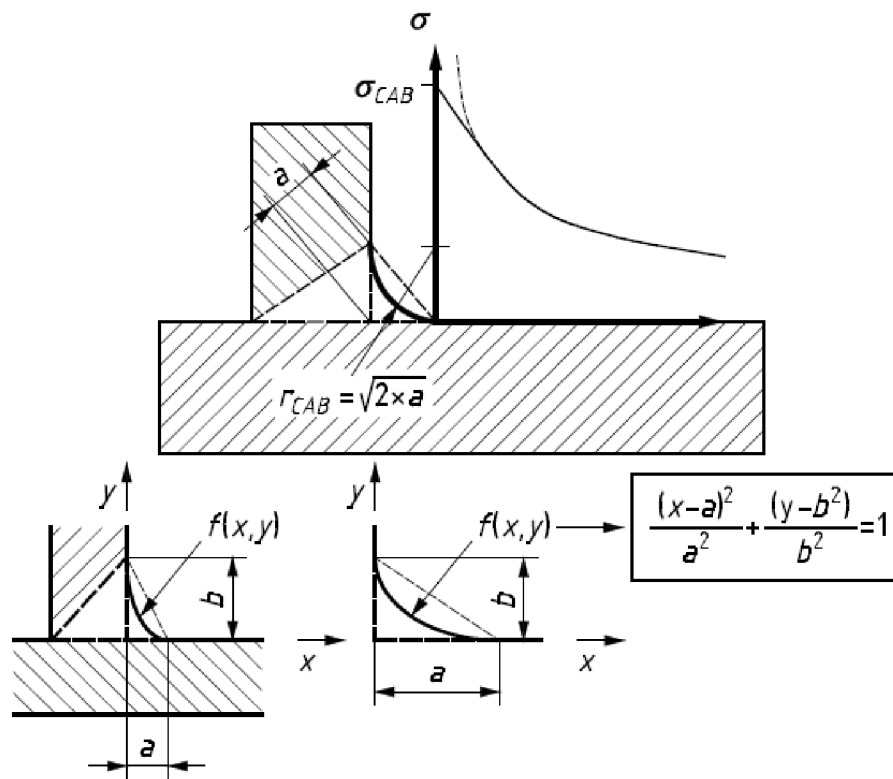


Figure 3.24: Through-wall linearization across the cross section at the weld toe (hot-spot)[10]

## 3.5.2.4. CAB-concept

Here, the fillet weld is replaced by a fictitious one to remove the sharp transition (notch effects) as in Figure 3.25. Generally, the fillet of the weld can always be realized by a spline approximation, tangentially to weld toes. In the case of  $45^\circ$  flank angles (flanks of the same length) the fillet can be modelled with the radius of a  $r_{CAB} = \sqrt{2} \cdot a$ . In the case of unequal flank lengths, as shown in the bottom Figure, the fillet shape can be approximated using an ellipse equation. [10]

Structural stress can then be analysed directly at the weld toe. When the stress determination is based on extrapolation methods the stress value in extrapolation points, in the case of inappropriate meshing, can be influenced by the weld (this especially applies to thin-walled structures). By using the CAB-method these uncertainties can be avoided due to the removal of the sharp notch in the geometry of the model. [10]



**Figure 3.25:** Approximation of the fillet weld by a spline according to the CAB-concept [10]

Because the CAB-method tends to give slightly conservative results, the stress which was determined by this method can be reduced for the testing group 1 or 2, for full penetration welds and for mechanical loads by a coefficient  $f_{CAB} = 0.95$ . [10, 8] Together with the Haibach method these are recommended approaches for structures where the thermal stresses also occur. Such analysis should always be realized using solid elements. [10]

3.5.2.5. Haibach–concept

In stress determination according to Haibach the structural stress is commonly measured in the distance of 2–3 mm from the weld toe. This is shown in Figure 3.26. However, in some thin-walled structures these distances could lead to non-conservative results. Hence, for structures which have their wall thickness under 8.0 mm the recommended distance from the weld toe is  $0.25 \cdot t$ . [10]

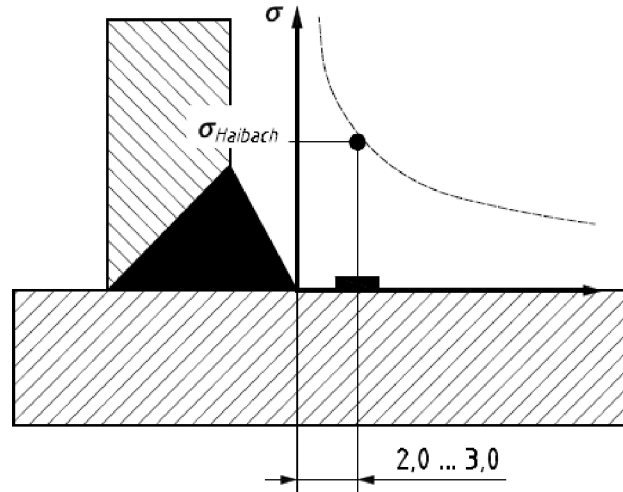


Figure 3.26: Hot-spot stress determination according to the Haibach concept [10]

For the fatigue assessment which uses the Haibach method the correction factors  $f_{ew}$  and  $f_w$  (see 3.2) should be equal to 1. [10]



### 3.5.3. Effective Notch Stress Approach

The effective notch stress approach is covered in the IIW recommendations for fatigue assessment as an alternative method which is applicable only when using FEA. [25] Here, it is assumed that the weld geometry is already known unlike when using the hot-spot and nominal approaches where the weld geometry is considered as a random variable affecting the resistance to fatigue. [15] The effective notch stress (see Fig. 3.19) includes notch effects at the weld roots as well as the weld toes. Both previously mentioned effects of notches might be responsible for a lower fatigue life of welded joints. To be able to incorporate various weld shape parameters, and nonlinear stress behaviour resulting from them, the actual weld radius is replaced by an effective value of  $r = 1$  mm (see Fig. 3.27) which has been verified to give consistent results. [2] This applies to common welds with the thickness of 5 mm and more. Thinner metal sheets with small weld seams require reduced reference radii ( $r = 0.3$  mm, eventually 0.05 mm). Using the reference radius together with an assumption of linear elastic behavior of the material means that the effective notch stress can be calculated. For the fatigue life assessment, only one S–N curve is enough for each material (steel, aluminum, etc.) and basic loading conditions (e.g. pure normal or shear stresses along weld). This makes the calculation of welded joints standardized. [25]

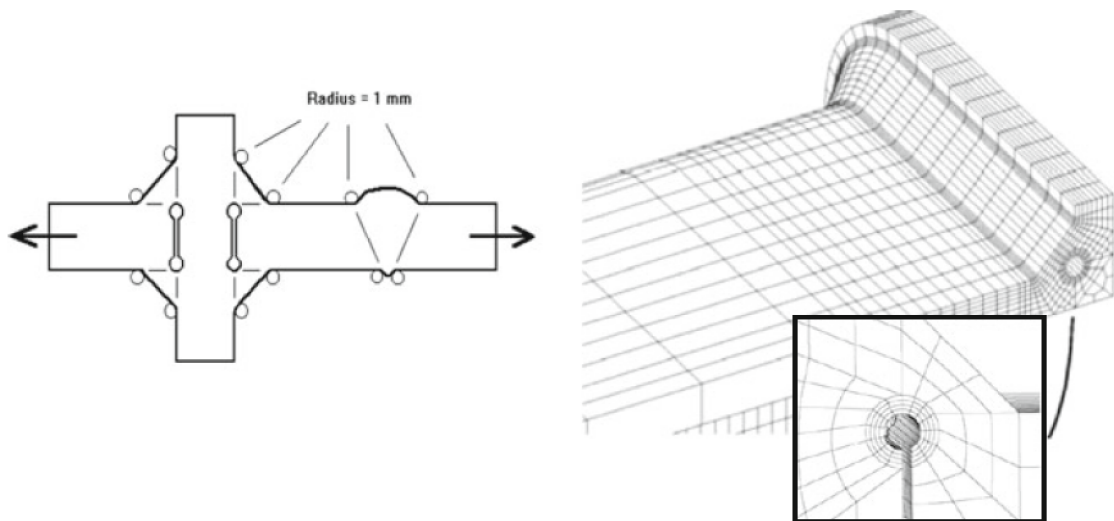


**Figure 3.27:** Effective radius of weld toes and roots (left) and a model example of FEA (right) [24]

When FEA is used for the welded joints fatigue analysis, it should be guaranteed that the mesh around stress-raisers is sufficiently fine to be able to capture the maximum stress values possible. According to [2], element sizes should not be bigger than  $1/6$  of the effective radius when linear elements are used and  $1/4$  of the effective radius in the case of quadratic (higher order) elements. The method does not cover crack growth of embedded defects that are initiated from surface roughness. *"The method is also not applicable if there is a significant stress component parallel to the weld."* [2] Further information on effective notch stress calculations can be found for example in [13] and [2].

## 4. Practical Part

In this chapter the fatigue assessment of the shell/nozzle junction<sup>1</sup> based on approaches described in the theoretical part will be presented. The model was done in SolidWorks [28]. The subsequent FEAs were carried out in Ansys [26] and evaluated according to the recent amendment of EN 13445-3 [10]. The auxiliary calculations were made in Matlab [27].

### 4.1. Vessel Geometry and Parameters

The inspected vessel is based on a real product that works as an air receiver in a production hall. The dimensions and the simplified shape of the air receiver are shown in Figures 4.1 and 4.2 below. Here, only the dimensions relevant to the evaluated detail are shown. Other design parameters which are relevant for the assessment procedure are given in Table 4.1 on the next page.



**Figure 4.1:** Solidworks model of the simplified vessel geometry

---

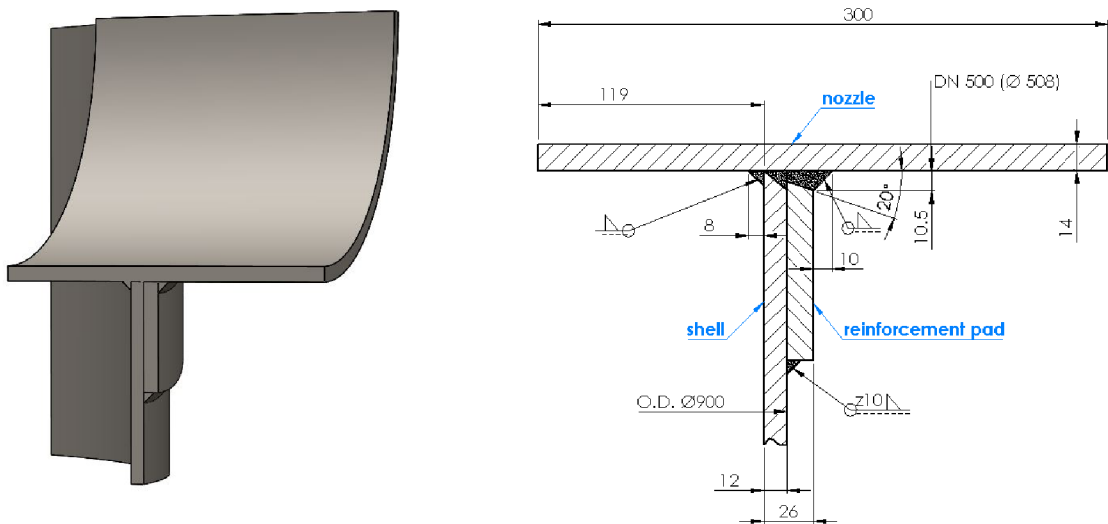
<sup>1</sup>The specification of the air receiver's geometry is further described in this chapter

**Table 4.1:** Technical parameters of the vessel

Technical parameters of the vessel		
pressure cycle	3 – 2.5	MPa
calc. temperature	35	°C
medium	pressurized air	—
material (shell, nozzles, reinforcement pad)	P265GH	—
material (legs)	S235JR	—
corrosion allowance	0	mm
test group	3	—

Figure 4.2 shows the detail of the geometry in the shell/nozzle junction including its dimensions and weld types. In the left figure, a section of the inspected area is shown. The area involves the nozzle, the reinforcement pad and a certain part of the vessel's shell. Figure on the right represents a drawing of the corresponding cross-section.

In the model, the materials of the welds and the body of the vessel are assumed to be the same. Generally, the welding material must always be of a higher quality than the parent material. For the assessment purposes, the weld cross-sections in Figure 4.2b) can be assumed as triangular.



(a) 3D model of the junction

(b) Drawing of the junction

**Figure 4.2:** Detail of the shell/nozzle junction



## 4.2. Application of FEA and Fatigue Analyses

The finite element analyses introduced in this section are based on the methods described in 3.5. Two different types of FEA were performed in Ansys. In the first analysis, the simulations were done with shell element models and in the second analysis with solid elements. All the simulations assume linear–elastic behaviour of the material (see 3.5).

All the stress determination methods evaluated and compared in the thesis according to the element type used are listed below:

- Shell element model
  - Linear surface extrapolation
  - Quadratic surface extrapolation
- Solid element model
  - Linear surface extrapolation
  - Quadratic surface extrapolation
  - Linearization
  - CAB–concept
  - Haibach–concept

Figure 4.3 shows a diagram of the analyses performed including the development process. The blue curve represents the shared material settings for all the analyses. The cyan curve represents the relation between the solution of the shell model and the boundary conditions of the solid submodels. This relation will be explained more closely in 4.2.2.

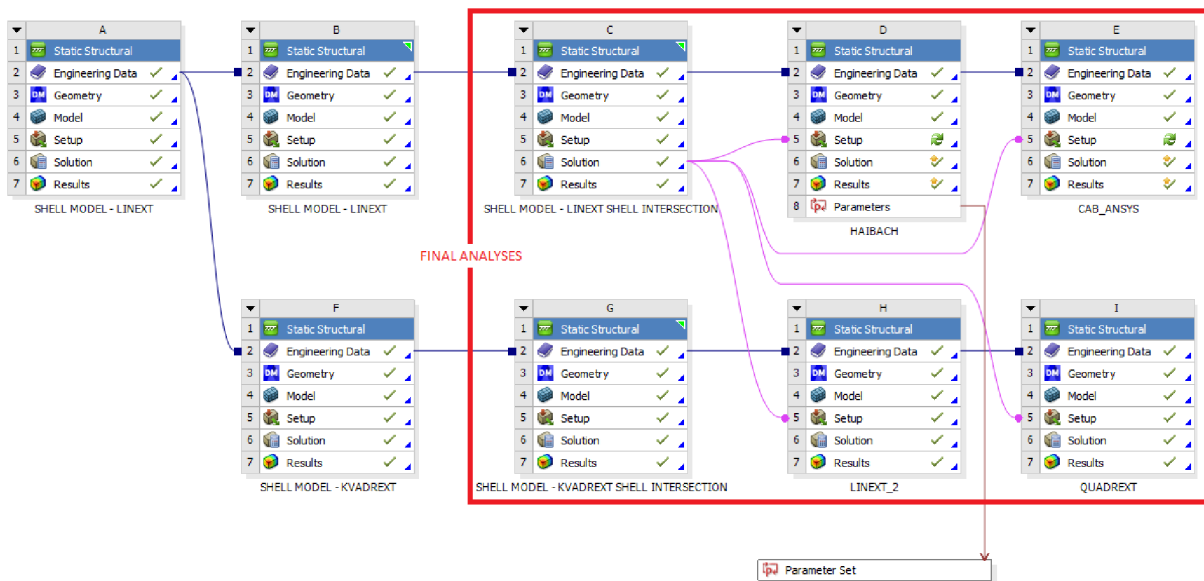


Figure 4.3: Diagram of the Ansys project

### 4.2.1. Shell Model

Here, the preparation process for the subsequent analysis of the shell element model will be outlined.

#### 4.2.1.1. Geometry

For both cases (shell and solid), the models were imported as Parasolid (.xt) files. The shell model was created from mid-surfaces of the model shown in Fig. 4.1. Then, the appropriate thicknesses of the components were added. The values of these thicknesses are only used to incorporate the stiffnesses of all components in the calculations and do not assign any actual thickness to the components. The shell model as well as the fictitious thicknesses are shown in Figure 4.4.

In [10], it is recommended to extrapolate towards the shell intersection for the shell element analysis. Here the weld details are not incorporated into the model.

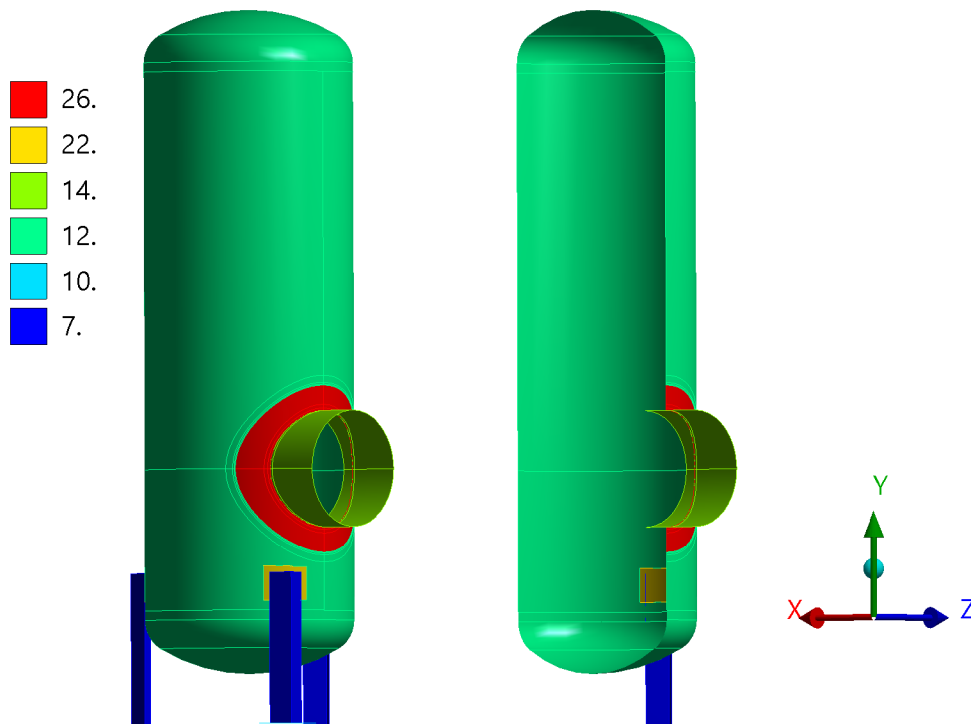


**Figure 4.4:** Shell model in Ansys (the individual colours represent thicknesses in mm)

The examined detail was divided into four sections and the reference points were placed along the boundaries of these sections. In addition to that, the paths for the evaluation of the stresses along the nozzle's periphery were included in the models. Figures 4.5 and 4.6 on the next page show the detail of the shell/nozzle junction with two and three reference points for the purposes of the linear and quadratic extrapolations, respectively.

#### 4.2. APPLICATION OF FEA AND FATIGUE ANALYSES

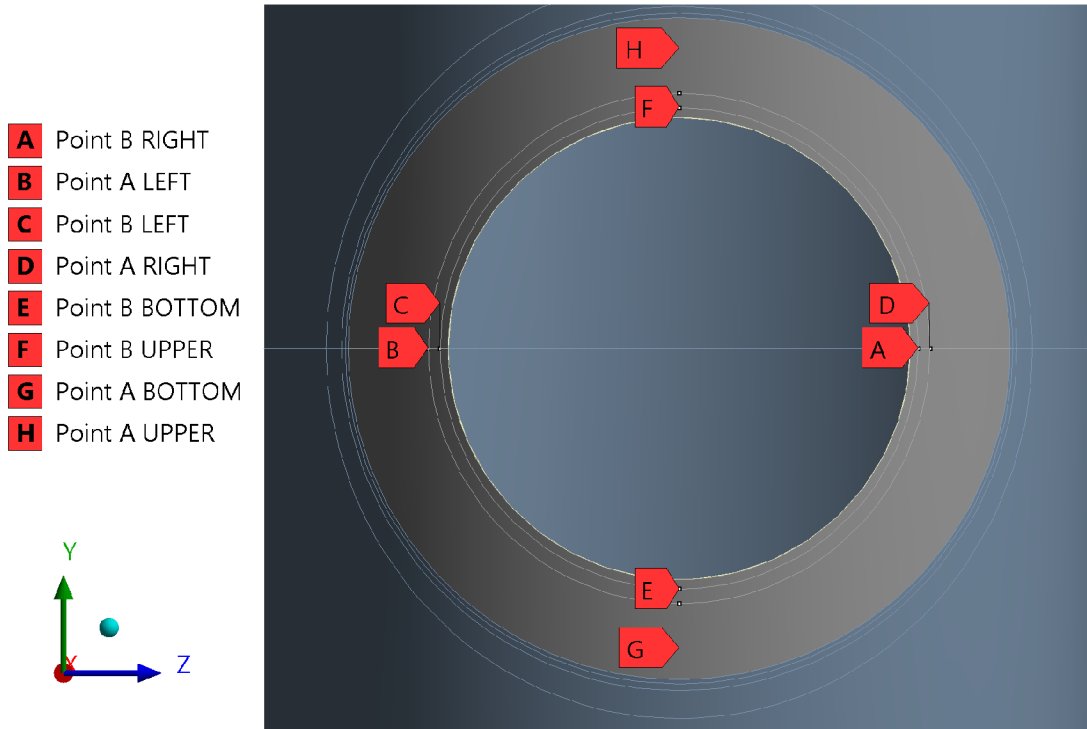


**Figure 4.5:** Shell/nozzle junction with reference points and paths for the linear extrapolation

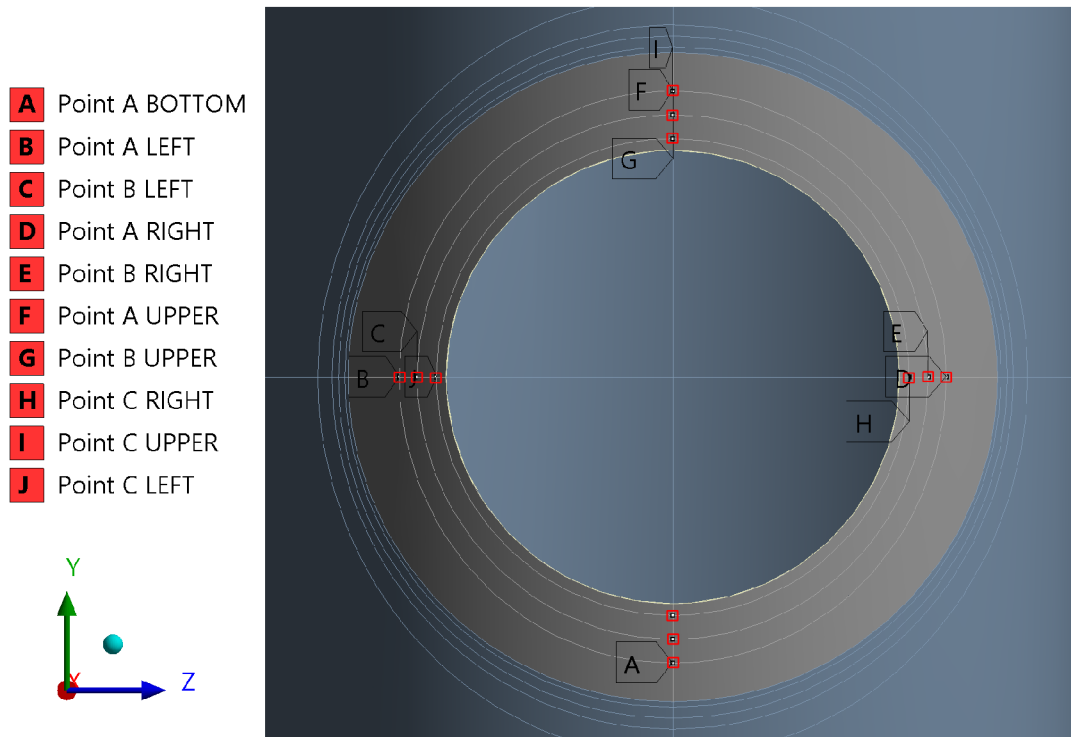


**Figure 4.6:** Shell/nozzle junction with reference points and paths for the quadratic extrapolation

#### 4.2.1.2. Mesh

The mesh shown in Figure 4.7 was created in accordance with the recommendations and guidelines described in the theoretical part of this thesis. The nodes of the adjacent elements are located in the reference points and on the paths along the nozzle. A finer mesh was set around the closest area of the intersection to get better accuracy.

To obtain the result shown below, more advanced techniques were used such as various sizing methods including the selective meshing which uses mesh recording. Since these more complicated settings would have no significant effect when applied on the model as a whole, most of them were primarily used only in the area of interest.

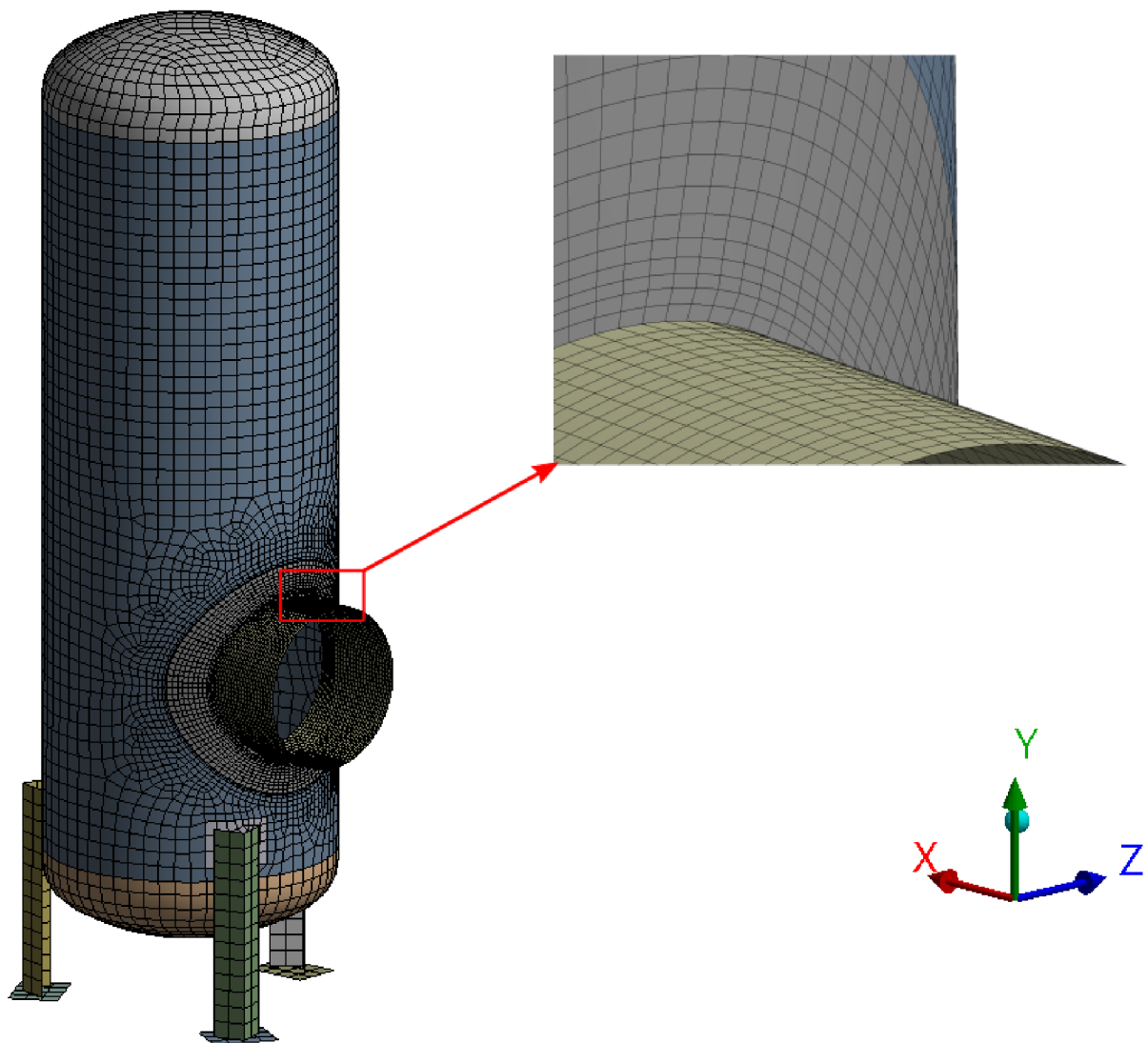


**Figure 4.7:** Appropriate mesh for the subsequent analysis of the shell model

## 4.2. APPLICATION OF FEA AND FATIGUE ANALYSES

### 4.2.1.3. Boundary Conditions and Mechanical Loads

The boundary conditions for the shell model were applied only to the anchor plates as shown in Figure 4.8. The used fixed supports restrict all degrees of freedom.

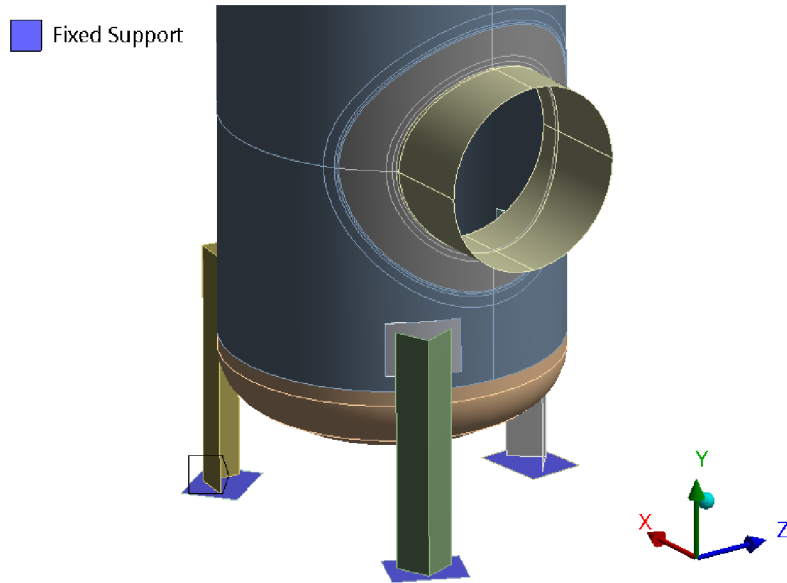


**Figure 4.8:** Boundary conditions of the shell model

The applied loads were as follows: the internal pressure  $p = 3 \text{ MPa}$  and the force along the nozzle opening calculated as:

$$F = p \cdot S_{nozzle} = p \cdot \pi R^2 = 3 \cdot 10^6 \cdot \pi \cdot 0.247^2 = 575 \text{ kN} \quad (4.1)$$

The force applied to the nozzle end is illustrated in Figure 4.9.

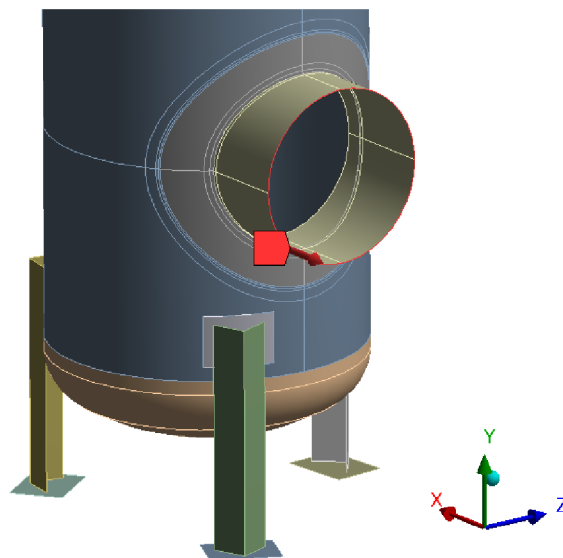


**Figure 4.9:** Force simulating the pressure on the flange

The effect of gravity on the structure was calculated in separate analysis and due to negligible resulting stresses, it was omitted in further analyses.

#### 4.2.1.4. FEA Associated Problems

This section will present and discuss the inaccuracies of the shell model which can have impact on the results.

One of the problems to address is the evaluation paths for the extrapolation (see Figures 4.5 and 4.6). These paths were chosen to be ellipses (a simplification of the real paths represented by 3D splines). The most significant difference between the real 3D splines, which are the result of the curved surface, and the simplified ellipses used for the analysis occurs at the  $45^\circ$  angle in all quadrants shown in Figure 4.10. This results in an error in the surface distances measured between the ellipses and the intersection of the nozzle and the shell. The error was determined to be approximately 5 % at the point of the greatest deviation (represented by the red line in Figure 4.10).

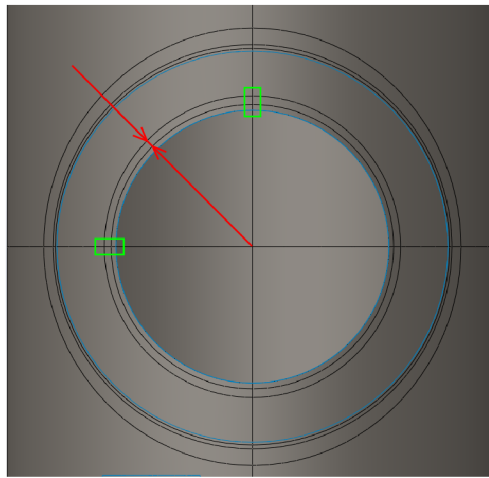


**Figure 4.10:** Deviation in the distance along the surface between evaluation paths

Figure 4.11 shows another phenomenon which can cause inaccuracies. Because the model consists only of shell elements, the attachment points of the legs and welding plates are located on the same mid-surface as is the shell. In the case of the welding plates, this can be solved by adding an offset to the mid-surface. However, this cannot be done in the case of the L-profiles. Since the L-profiles are connected only to the welding plates, the stiffness should not be affected. Therefore, it is possible that the overlaps shown below can be only an error in display.

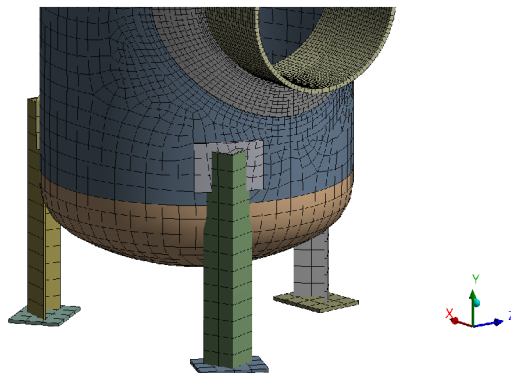


**Figure 4.11:** Possibly problematic connection of parts

### 4.2.2. Solid Model

Since the FEAs which use solid elements are generally computationally expensive, it is advantageous to use so-called sub-modeling techniques. Using sub-modeling can save a large amount of time when a specific part of the model needs to be analyzed in detail. Here, only the main subject of interest (the shell/nozzle junction) is modeled using solid elements. The solid sub-model shares the coordinate system with the global model. The boundary conditions are taken from the global shell model of the vessel. In Ansys, this is done by loading the solution of the global model into the setup of the sub-model (see Fig.4.3). The principles of sub-modeling are shown in Figure 4.12.

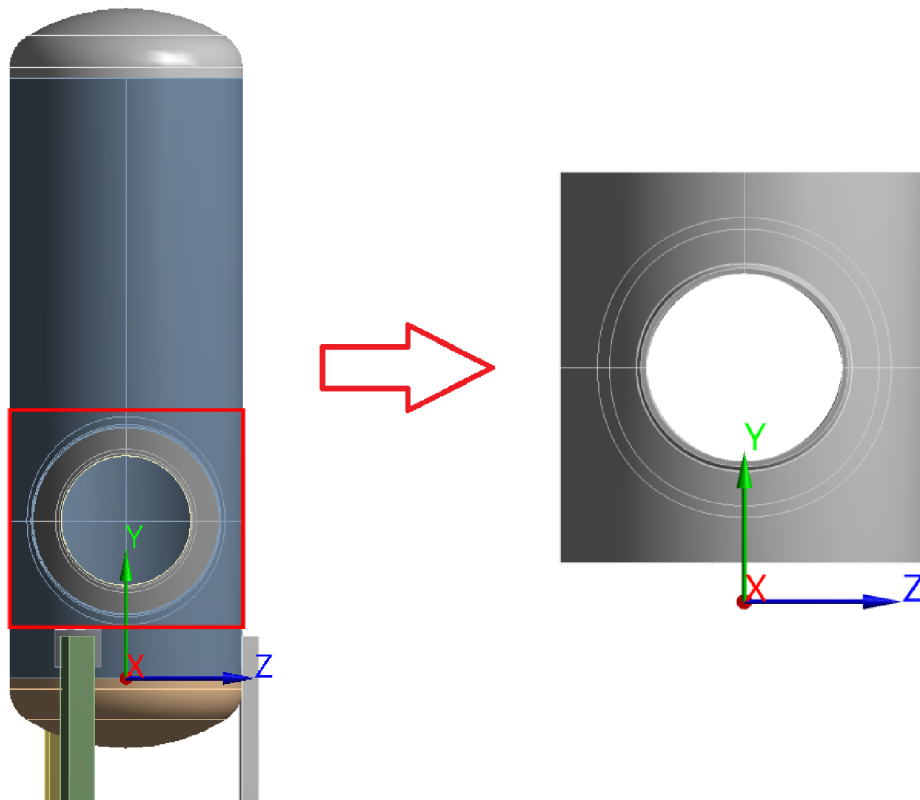


Figure 4.12: Shell to solid sub-modeling

#### 4.2.2.1. Geometry

Solid-element sub-models were imported from SolidWorks without any additional geometry settings (only, corrections of the imported geometry had to be made which are described in section 4.2.2.4). Here, the welds are already fully incorporated into the models. The geometry remains the same for all analyses. For the CAB-method, however, a slight adjustment of the weld seam had to be made. The reference points and paths for the evaluation in solid-element models were set up in a similar way as in the case of the shell-element models (see 4.4).

The models for the evaluation according to the Haibach (which has identical geometry to the other sub-models) and CAB methods are shown in Figures 4.13 and 4.14. Figures for the other analyzed methods can be found in Attachment 2.



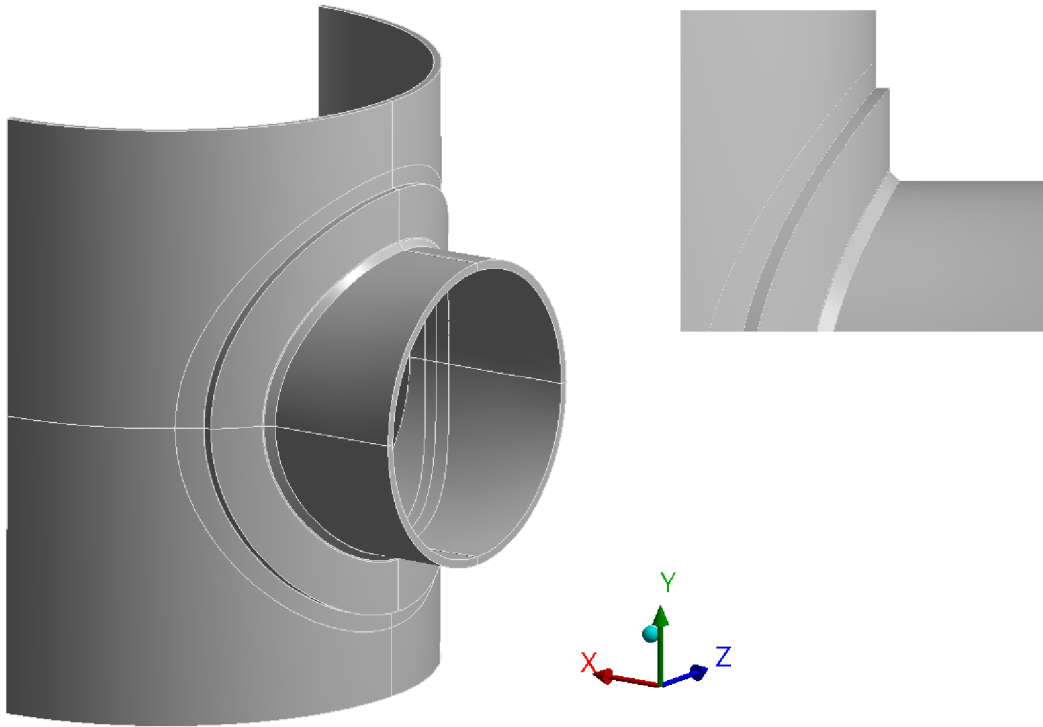


**Figure 4.13:** Geometry of sub-models with a triangular weld, here represented by a model according to the Haibach method

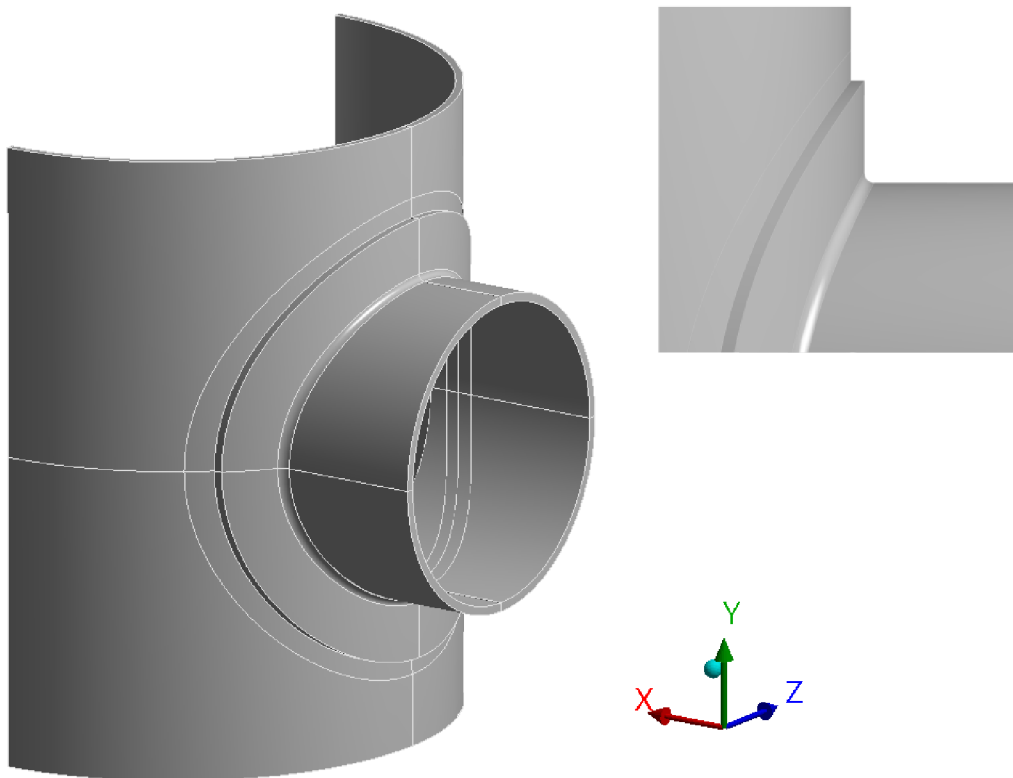


**Figure 4.14:** Geometry according to the CAB-method with a fillet radius

## 4.2. APPLICATION OF FEA AND FATIGUE ANALYSES

### 4.2.2.2. Mesh

The meshes for both the solid–element and shell models were constructed according to the principles detailed in the theoretical part.

More advanced techniques were used for the meshing of the entire sub–model. Single bodies of the sub–model always have three elements across their thickness. This number should be sufficient for obtaining satisfactory stress results from the subsequent analysis. Because solid–element model analyses are usually computationally expensive, optimization of the mesh is crucial. Figure 4.15 shows an example modeled according to the Haibach method. The elements on the boundary of the sub–model are relatively large and get smaller towards the weld seam. This behaviour is advantageous because the number of elements is relatively small while still giving good results in the inspected area.

To get a result as satisfactory as in Figure 4.15, significantly more time was needed for the mesh preparation compared to the case of the shell–element model.

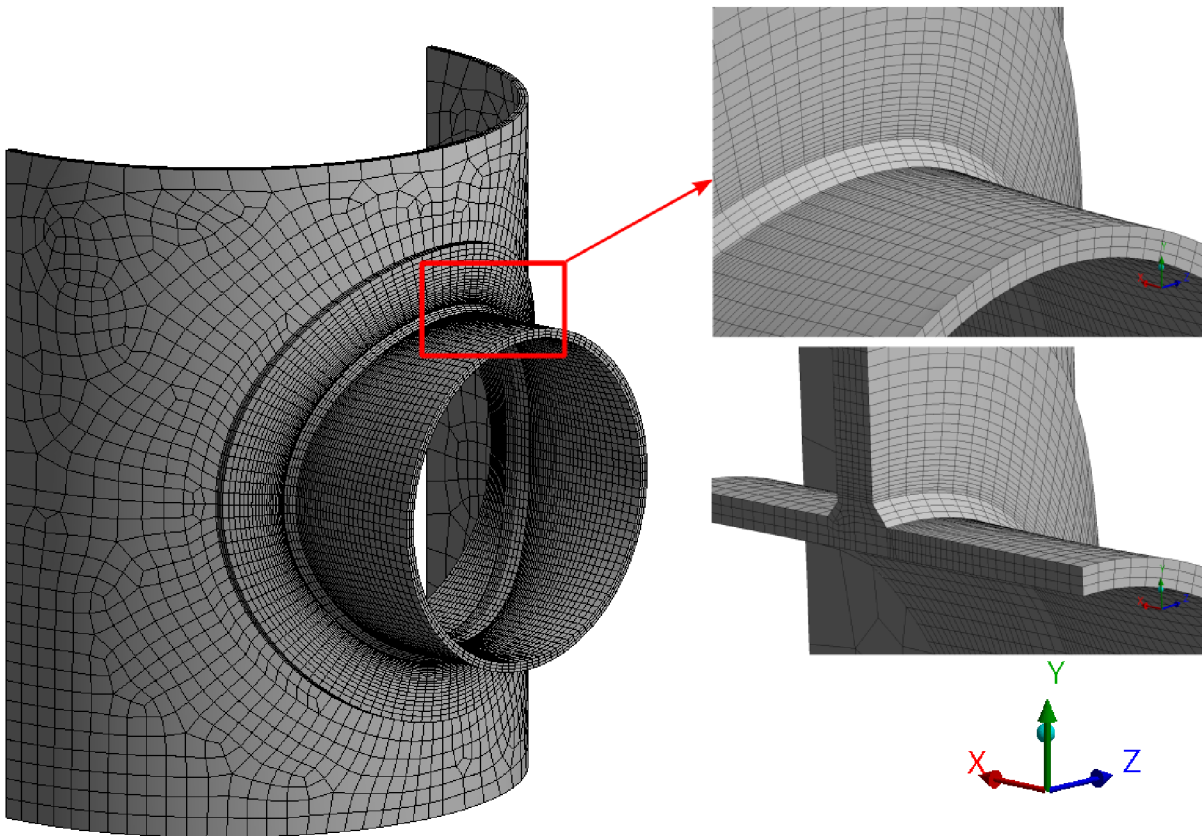


**Figure 4.15:** Appropriate mesh for the subsequent analysis of the solid submodel

#### 4.2.2.3. Boundary Conditions and Mechanical Loads

Here, the boundary conditions are represented by the imported displacements from the global shell model. These are applied on the faces along the sub-model's boundaries as shown in Figure 4.16.

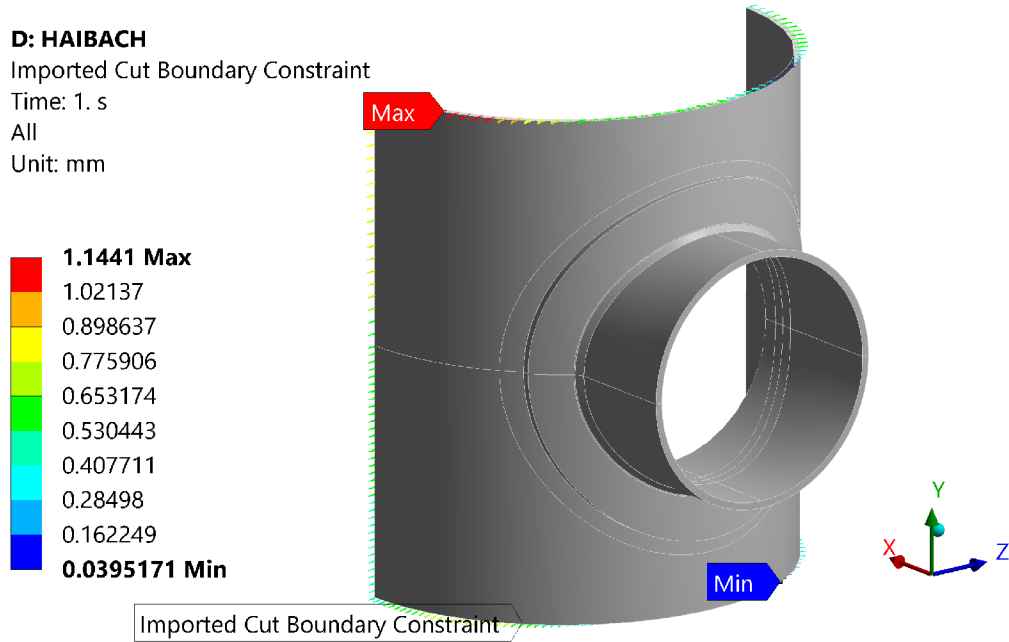


**Figure 4.16:** Appropriate mesh for the subsequent analysis of the solid submodel

The same loads were applied to the shell element model as well as to the solid element sub-model: the internal pressure  $p = 3 \text{ MPa}$  and the force  $F = 575 \text{ kN}$ . The force applied to the end of the nozzle is illustrated in Figure 4.17.

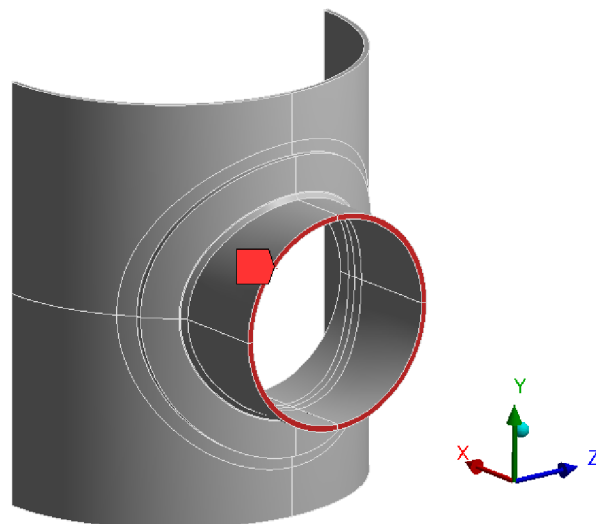


**Figure 4.17:** The tensile force at the nozzle end of the submodel

## 4.2. APPLICATION OF FEA AND FATIGUE ANALYSES

### 4.2.2.4. FEA Associated Problems

The problems regarding the evaluation paths described in 4.2.1.4 are also present in the solid–element models. Here, the error determined at the point of the greatest deviation is approximately 5 % as well.

In the solid–element analyses, the biggest struggle occurred in the imported geometry. The models in SolidWorks had very slight overlaps or gaps between adjacent bodies which subsequently caused unexpected problems in Ansys. This happened primarily in the areas of adjacent bodies on curved surfaces or between bodies created by slicing. In Ansys, these tiny inaccuracies (usually around  $10^{-4}$ – $10^{-3}$  mm) resulted in unmeshable volumes. This can be corrected by connecting the problematic bodies via so–called contacts and not via shared topology. However, the analyses of bodies connected through this approach do not give reliable results in these contacts. In this case, such approach was not desirable. With some effort though, it was possible to repair the SolidWorks models by partial remodeling. After the import and creation of the shared topology in Ansys some edges and faces of the models fell apart. Finally, this was solved by creating virtual cells over the problematic entities.

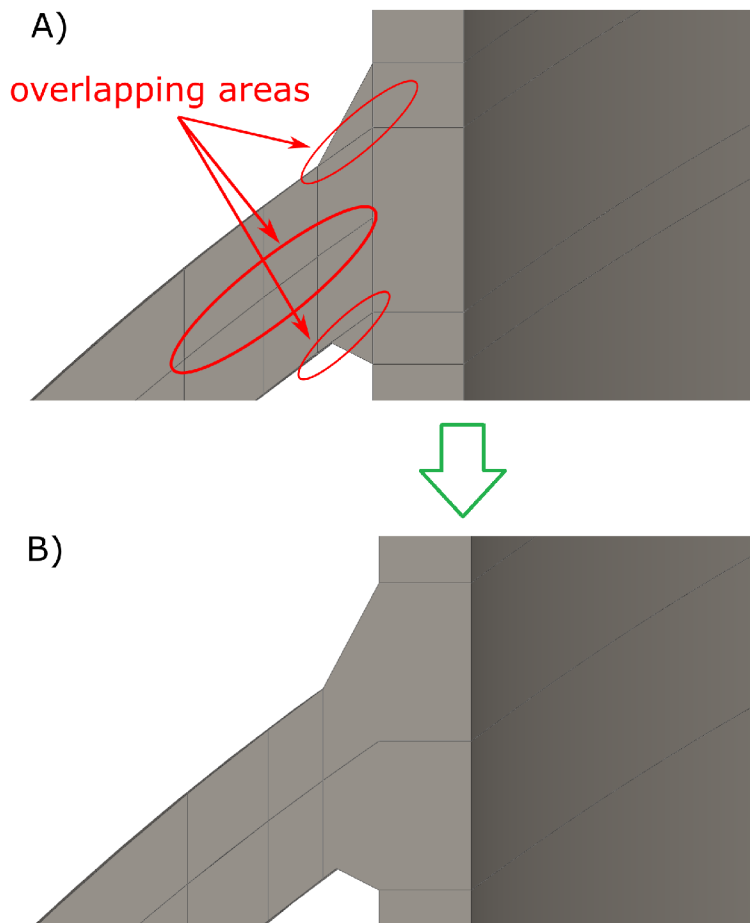


**Figure 4.18:** Section of one of the sub–models in SolidWorks:  
a) model with overlapping bodies; b) repaired model (partially remodelled)

### 4.3. Final Evaluation and Results

Here, the final assessment of the fatigue life will be introduced. Also, the stress evaluation approaches will be compared in the reference points shown in Figure 4.19. The results will be then discussed in the conclusion.

The calculation of the fatigue life was performed according to [10]. The procedure was described in detail in Section 3.2.1 of the theoretical part. For the inspected structural detail (shell/nozzle junction), the following applies:

**Table 4.2:** The assigned fatigue class given in Table 18–7 of [10]

Joint type	Class	$\Delta\sigma_D$ [MPa]	$\Delta\sigma_{Cut}$ [MPa]
weld toe in shell	63	46	26

Since the thickness correction factor  $f_w$  is for all examined cases approximately equal to 1, we can assume that  $\frac{\Delta\sigma_R}{f_w} \approx \Delta\sigma_R$ . Then, according to Table 4.2, getting stress ranges from FEA of lower values than  $\Delta\sigma_D$  will ensure (in the studied case) the number of life-cycles approaching infinity.

Since the performed analyses are based on linear-elastic material behaviour and the deformations are small, the acting stresses should also behave linearly. Therefore, to obtain the equivalent stress range, the stress in the maximum of the loading cycle can be simply multiplied by the min/max ratio and then subtracted from the original value. For each stress evaluation method, the stress ranges and the calculated numbers of allowable life cycles are listed in Tables 4.3 and 4.4.

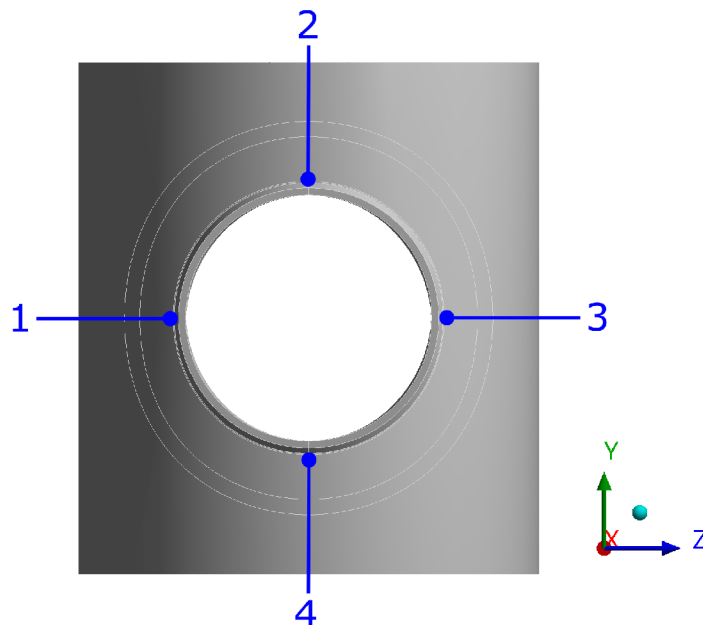


**Figure 4.19:** Reference points for the comparison of the stress determination methods

### 4.3. FINAL EVALUATION AND RESULTS

**Table 4.3:** Shell–element model analysis results

SHELL MODEL	$\Delta\sigma_{eq}$ [MPa]					Allow. cycles
	1	2	3	4	Along the path	
Reference points	1	2	3	4	Along the path	N
Linear extrapolation	16.24	44.88	16.45	45.70	47.65	4.87 mil.
Quadratic extrapolation	17.72	44.39	18.54	46.18	49.51	4.00 mil.

**Table 4.4:** Solid–element model analysis results

SOLID MODEL	$\Delta\sigma_{eq}$ [MPa]					Allow. cycles
	1	2	3	4	Along the path	
Reference points	1	2	3	4	Along the path	N
Linear extrapolation	17.90	32.77	18.02	33.53	33.56	Infinite
Quadratic extrapolation	17.78	37.50	18.60	34.40	34.18	Infinite
Linearization	16.52	33.15	16.81	33.71	—	Infinite
CAB–concept	16.60	34.48	16.82	35.17	34.19	Infinite
Haibach–concept	18.51	32.31	18.96	33.12	33.12	Infinite

The values in Tables 4.3 and 4.4 were calculated using Matlab. The "Along the path" results represent the maximal stress ranges acquired from the nodes on the evaluation paths described in 4.2. To get these values by extrapolation, a Matlab script was written (example in Attachment 1). The stress components in the nodes located on the paths used for the extrapolation were saved into datasheets and imported as matrices to Matlab. Then, the corresponding elements of these matrices were extrapolated and stored in the matrix of extrapolated stress components. From these components, the resulting stresses in the nodes (their maxima) were calculated. Finally, the script finds the specified  $k$  number of maximum stress values and their locations on the evaluation path.

## 5. Conclusion

This diploma thesis presented stress determination approaches which use FEA introduced in Annex NA of the recent draft amendment to Clause 18 of EN 13445-3 and which may be implemented into EN 13445-3 [11] in the nearest future. These approaches were used in the fatigue assessment of the shell/nozzle junction of the given pressure vessel.

The fatigue assessment was carried out for two models to use all the stress evaluation methods introduced in [10]. The first model consisted of shell elements and the second one of solid elements. These models were created in SolidWorks and analyzed in Ansys. However, it has become clear that SolidWorks was not ideal for very precise modeling which was necessary in this particular case. Even though the part was modeled properly, there were inaccuracies between some of the adjacent bodies. After the import of the geometry into Ansys these inaccuracies caused serious problems which had to be resolved using repair features and sometimes even partial remodeling (Chapter 4.2.2.4).

The performed analyses were well feasible and they all gave similar results. The results can be found in Chapter 4.3 of the practical part. The analysis performed on the shell–element model tends to give more conservative results compared to the solid–element model. The quadratic surface extrapolation is preferred over the linear extrapolation in shell–element model analysis. This is because the quadratic function represents the actual increase of the stress better. Generally, shell models are less accurate but simpler and less computationally expensive. This makes the FEA which uses shell elements a suitable method for non–critical applications.

In the case of solid–element models, the Haibach method or the CAB method seem to be the best option, mainly because of the easier pre– and post–processing. Linearization would also be a good choice for the evaluation of stresses in the reference points. In Ansys however, the evaluation of the linearized stresses along the reference path around the nozzle cannot be done easily.

Finally, it was discovered that the recommendations for the stress determination methods in [10], Annex NA, are not precisely defined in some cases. The actual shape of the weld changes along its length around the nozzle. This can influence the stress values on the given evaluation paths to some extent. In [10], no recommendations are given regarding this problem. Also, there are no explicit rules for the incorporation of the weld stiffness in the shell models. For further information, it usually refers to the IIW recommendations and other references. In practice however, this devalues the intended user–friendliness of the Annex NA.



## 6. Bibliography

- [1] JIA, Junbo. 2014. *Essentials of Applied Dynamic Analysis* [online]. Heidelberg: Springer. Available at: <https://www.springer.com/gp/book/9783642370021>
- [2] HOBACHER, A.F. 2016. *Recommendations for Fatigue Design of Welded Joints and Components* [online]. 2. Switzerland: Springer International Publishing. Available at: <https://www.springer.com/gp/book/9783319237565#aboutBook>
- [3] ERIKSSON, Å. 2003. *Weld evaluation using FEM - A guide to fatigue-loaded structures*. 1. Gothenburg, Sweden: Industrilitteratur AB.
- [4] MUGHRABI, Haël. 2015. *Microstructural mechanisms of cyclic deformation, fatigue crack initiation and early crack growth*. Phil. Trans. R. Soc. A. 373(2038).
- [5] EERME, Martin. *Fatigue overview* [online]. Tallin: Tallinn University of Technology, Faculty of Mechanical Engineering, 92 p. Available at: [http://innomet.ttu.ee/martin/Mxx0060/Fatigue\\_overview.pdf](http://innomet.ttu.ee/martin/Mxx0060/Fatigue_overview.pdf). Study materials.
- [6] SAN MARCHI, C., D.E. DEDRICK, P. VAN BLARIGAN, B.P. SOMERDAY and K.A. NIBUR. 2011. *PRESSURE CYCLING OF TYPE 1 PRESSURE VESSELS WITH GASEOUS HYDROGEN* [online]. Sandia National Laboratories, 12 p. Available at: [https://h2tools.org/sites/default/files/2019-08/paper\\_148.pdf](https://h2tools.org/sites/default/files/2019-08/paper_148.pdf)
- [7] SCHIJVE, J. 2009. *Fatigue of Structures and Materials* [online]. 2. Dordrecht: Springer. Available at: <https://www.springer.com/gp/book/9781402068072>
- [8] RUDOLPH, J., G. BAYLAC, R. TRIEGLAFF, R. GAWLICK, M. KRÄMER, Y. SIMONET and M. TRIAY. 2019. Outline of the recent consolidated revision of EN13445-3, clause 18 and related annexes: detailed assessment of fatigue life. *Procedia Structural Integrity* [online]. 19, 575-584. Available at: <https://linkinghub.elsevier.com/retrieve/pii/S245232161930530X>
- [9] TRIEGLAFF, Ralf, Jürgen RUDOLPH, Martin BECKERT, Daniel FRIERS and G. HÉNAFF. 2018. Methods for Structural Stress Determination according to EN 13445-3 Annex NA – Comparison with other Codes for Unfired Pressure Vessels. *MATEC Web of Conferences* [online]. 165. Available at: <https://www.matec-conferences.org/10.1051/mateconf/201816510003>
- [10] CEN/TC 54. 2019. *Unfired pressure vessels – Part 3: Design; German and English version EN 13445-3:2014/prA20:2019*. Brussels: CEN-CENELEC.
- [11] CEN/TC 54. 2018. *Unfired pressure vessels – Part 3: Design; German version EN 13445-3:2014*. Brussels: CEN-CENELEC.
- [12] NIEMI, E., Wolfgang FRICKE and S. J. MADDOX. 2018. *Structural Hot-Spot Stress Approach to Fatigue Analysis of Welded Components: designer's guide* [online]. 2. Singapore: Springer. Available at: <https://www.springer.com/gp/book/9789811055676>

- [13] BRUDER, T., K. STÖRZEL, J. BAUMGARTNER and H. HANSELKA. 2012. Evaluation of nominal and local stress based approaches for the fatigue assessment of seam welds. *International Journal of Fatigue* [online]. 34(1), 86-102. Available at: <https://linkinghub.elsevier.com/retrieve/pii/S0142112311001447>
- [14] HOBACHER, A. 2009. The new IIW recommendations for fatigue assessment of welded joints and components – A comprehensive code recently updated. *International Journal of Fatigue* [online]. 31(1), 50-58. Available at: <https://linkinghub.elsevier.com/retrieve/pii/S0142112308001072>
- [15] NIEMI, Erkki (ed.). 1995. *Stress Determination for Fatigue Analysis of Welded Components*. 1. Cambridge: Abington Publishing.
- [16] AYGÜL, MUSTAFA. 2012. *Fatigue Analysis of Welded Structures Using the Finite Element Method*. Gothenburg, Sweden. Diplom thesis. Chalmers University of Technology, Department of Civil and Environmental Engineering. Supervisor Mohammad Al-Emrani. Available at: <https://publications.lib.chalmers.se/records/fulltext/155710.pdf>
- [17] SHANDOOKH, Ahmed. 2016. *Experimental Study of Plasma Shot Peening and Laser Shock Peening on Mechanical Properties and Fatigue Life of a Certain Aluminum Alloys*. [online]. Iraq. Doctor thesis. University of Technology, Mechanical Engineering Department. Supervisor Dr.Hussain J.M. Al-Alkawi. Available at: [https://www.researchgate.net/publication/311900356\\_Experimental\\_Study\\_of\\_Plasma\\_Shot\\_Peening\\_and\\_Laser\\_Shock\\_Peening\\_on\\_Mechanical\\_Properties\\_and\\_Fatigue\\_Life\\_of\\_a\\_Certain\\_Aluminum\\_Alloys](https://www.researchgate.net/publication/311900356_Experimental_Study_of_Plasma_Shot_Peening_and_Laser_Shock_Peening_on_Mechanical_Properties_and_Fatigue_Life_of_a_Certain_Aluminum_Alloys).
- [18] Material Fatigue. 2017. In: *Multiphysics Cyclopedia* [online]. Available at: <https://www.comsol.eu/multiphysics/material-fatigue>
- [19] RICHARD, H.A. and M. SANDER. 2016. *Fatigue Crack Growth: Detect—Assess—Avoid* [online]. 1. Switzerland: Springer. Available at: <https://www.springer.com/gp/book/9783319325323>
- [20] M. M. Pedersen, 2018. *Introduction to Metal Fatigue*. [online]. Department of Engineering, Aarhus University. Denmark. 91 pp. - Technical report ME-TR-11 Available at: [https://www.researchgate.net/publication/329699083\\_Introduction\\_to\\_Metal\\_Fatigue\\_-\\_Concepts\\_and\\_Engineering\\_Approaches/link/5c1614f292851c39ebf0eaae/download](https://www.researchgate.net/publication/329699083_Introduction_to_Metal_Fatigue_-_Concepts_and_Engineering_Approaches/link/5c1614f292851c39ebf0eaae/download)
- [21] APPEL, M. 2013. *Modelování tenkostěnných rámců mechatronických soustav s koutovými svary a jejich vliv na vlastní frekvence* [online]. Brno. Bachelor thesis. Brno University of Technology. Supervisor Petr Vosynek. Available at: [https://www.vutbr.cz/studenti/zav-prace?zp\\_id=68593](https://www.vutbr.cz/studenti/zav-prace?zp_id=68593)
- [22] GÖRANSSON, Andréas. 2014. *Fatigue life analysis of weld ends: Comparison between testing and FEM-calculations* [online]. Linköping. Diplom thesis. Linköping University, Department of Management and Engineering, Division of Solid Mechanics. Supervisor Daniel Leidermark. Available at: <http://liu.diva-portal.org/smash/record.jsf?searchId=5&pid=diva2%3A734520&dswid=-7160>

- [23] Kalnins, A. 2008. *Stress Classification Lines Straight Through Singularities*. Chicago, Illinois USA. Paper PVP2008-61746. Proceedings of PVP2008, 2008 ASME Pressure and Piping Division Conference. Available at: <https://www.scribd.com/document/329398632/Asme-stress-Classification-Lines-Straight-Through-Singularities>
- [24] JONSSON, B., G. DOBMANN, A.F. HOBACHER, M. KASSNER and G. MARQUIS. 2016. *IIW Guidelines on Weld Quality in Relationship to Fatigue Strength* [online]. 1. Cham: Springer. Available at: <https://doi.org/10.1007/978-3-319-19198-0>
- [25] ROTHER, Klemens and Wolfgang FRICKE. 2016. Effective notch stress approach for welds having low stress concentration. *International Journal of Pressure Vessels and Piping* [online]. 147, 12-20. Available at: <https://linkinghub.elsevier.com/retrieve/pii/S0308016115300764>
- [26] *ANSYS® Academic Research Mechanical*. [Computer software].Release 19.2. Help System, Coupled Field Analysis Guide. ANSYS, Inc.
- [27] *MATLAB and Statistics Toolbox*. [Computer software].Release 2019b. The MathWorks, Inc., Natick, Massachusetts, United States.
- [28] *SOLIDWORKS 2018 Student Edition*. [Computer software].Release 2018. Dassault Systemes - SolidWorks Corporation, Massachusetts, United States.

# List of Abbreviations

FEA/FEM	Finite element analysis/ Finite element method
IIW	International Institute of Welding
S-N	Stress-number
$\sigma_a$	Stress amplitude
$\sigma_m$	Mean stress
$\sigma_{max}$	Maximal applied stress
$\sigma_{min}$	Minimal applied stress
$\Delta\sigma$	Stress range
$\Delta\sigma_{eq}$	Equivalent stress range
$\Delta\sigma_R$	Stress range obtained from fatigue design curve
$\Delta\sigma_D$	Endurance limit
$\Delta\sigma_{Cut}$	Cut-off limit
R	Stress ratio
$S_f$	Fatigue limit
N	Number of cycles
$n_i$	Specified number of cycles
C	Empirical constant of fatigue curves
m	Slope of a fatigue curve
e, t	Parent material thickness
$e_n$	Material thickness
$k_e$	Mechanical loading correction factor for plasticity
$D_f$	Cumulative fatigue damage index
$f_{ew}$	Thickness correction factor in welded components
$f_{T^*}$	Temperature correction factor
$f_w$	Overall correction factor applied to welded components
$f_{T^*}$	Temperature correction factor

$f_m$	Mean stress correction factor for unwelded material
$f_m^*$	Mean stress correction factor for fully stress relieved welded material
$T^*$	Assumed mean cycle temperature
$T_{max}$	Maximum operating temperature
$T_{min}$	Minimum operating temperature
$N_i$	Allowable number of cycles
F	Force
p	Pressure

# List of Attachments

1. Example of Matlab script used for extrapolation
2. Figures of solid element models for FEA
3. Stress intensity of shell and solid models

# Attachment 1

## Example of Matlab script used for extrapolation

---

```
clc; clear all; close all;
% Poradi bodu, zkontrolovat!
strings = ["C","B","A"];
% Pozice v tenzoru napeti
comps = ["X" "XY" "XZ";
         "XY" "Y" "YZ";
         "XZ" "YZ" "Z"];
% Cesty k souboru
base_path = "Point_";
base_ext = "exp_";
% Tloustka
t = 26;
% Vstupni data: body pro interpolaci
x1 = 0.5 * t;
x2 = 1 * t;
x3 = 1 * t;
x = [x1,x1+x2,x1+x2+x3];
% Pocet bodu na kruznici
num_elem = 121;
% Stupen polynomu
poly_dgr = 2;
% Prealokace pole pro tenzory
tensors{length(strings),num_elem} = [];
for i = 1:size(tensors,1)
    for j = 1:size(tensors,2)
        tensors{i,j} = zeros(3,3);
    end
end
% Projed body CBA
for i = 1:numel(strings)
    % Prealokace
    tens = zeros(3,3);
    % Projed cely tensor, zbytecne, ale funguje...
    for j = 1:3
        for k = 1:3
            path =
                strcat(base_path,strings(i),"\",base_ext,strings(i),\"_\",comps(j,k),\".txt\");
            num = readmatrix(path);
            nap = num(:,5);
            for b = 1:num_elem
                tensors{i,b}(j,k) = nap(b);
            end
        end
    end
end
end
```



```

% Vynasobeni 1/6
for i = 1:size(tensors,1)
    for j = 1:size(tensors,2)
        tensors{i,j} = tensors{i,j} * (1/6);
    end
end
% Prealokace
results{1,num_elem} = [];
for i = 1:size(results,2)
    results{i} = zeros(3,3);
end
% Spocitej odpovidajici tenzory v bode 0
for i = 1:num_elem
    T = tensors(:,i);
    results{i} = ext_nula(T,x,poly_dgr);
end
% Redukovane napeti
ds_result = zeros(1,num_elem);
for i = 1:num_elem
    [V1,D]=eig(results{i});
    sigma_1=max(diag(D));
    sigma_3=min(diag(D));
    ds_result(i)=sigma_1-sigma_3;
end
n = 3;
ds_result_sub = maxk(ds_result,n)
% Najdi indexy
ind = zeros(1,n);
for i = 1:n
    ind(i) = find(ds_result==ds_result_sub(i));
end

% Vypocitej redukovane napeti v odpovidajicich tenzorech
% Redukovane napeti
ds_other = zeros(size(tensors,1),n);
for i = 1:n
    for j = 1:size(tensors,1)
        [V1,D]=eig(tensors{j,ind(i)});
        sigma_1=max(diag(D));
        sigma_3=min(diag(D));
        ds_other(j,i)=sigma_1-sigma_3;
    end
end
ds_final = [ds_result_sub;
            ds_other];
x_ext = [0 x];
for i = 1:n
    figure(i)
    hold on
    polynom = polyfit(x_ext,ds_final(:,i)',poly_dgr);

```

```

% Funkcni hodnoty
plot(x_ext, ds_final(:,i)', 'o');
    grid on
% ---Zobraz cely polynom---
x_ext_poly = x_ext(1):0.01:x_ext(end);
y_ext_poly = polyval(polynom, x_ext_poly);
plot(x_ext_poly, y_ext_poly, 'r');
    grid on
end

%-----
function T4 = ext_nula(T,x,poly_dgr)
    for i = 1:numel(T{1,1})
        % ---Hodnoty x a y v bodech pro interpolaci---
        y = [];
        for j = 1:numel(T)
            y = [y T{j}(i)];
        end
        % Interpoluj, polynom druheho stupne
        polynom = polyfit(x,y,poly_dgr);
        % ---Nove body pro extrapolaci---
        x_ext = [0 x];
        % Nove funkci hodnoty na zaklade polynomu
        y_ext = polyval(polynom, x_ext);
        % ---Ulozit extrapolovana data do tenzoru--
        T4(i) = y_ext(1);
    end
    T4 = reshape(T4, [3,3]);
end

```

---

# Attachment 2

## Figures of solid element models for FEA

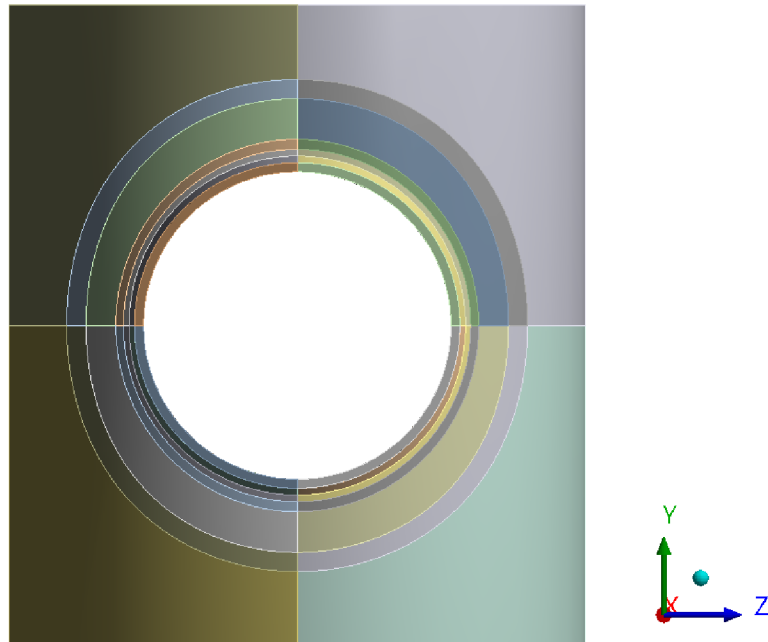


Figure 6.1: FEA model for linear extrapolation

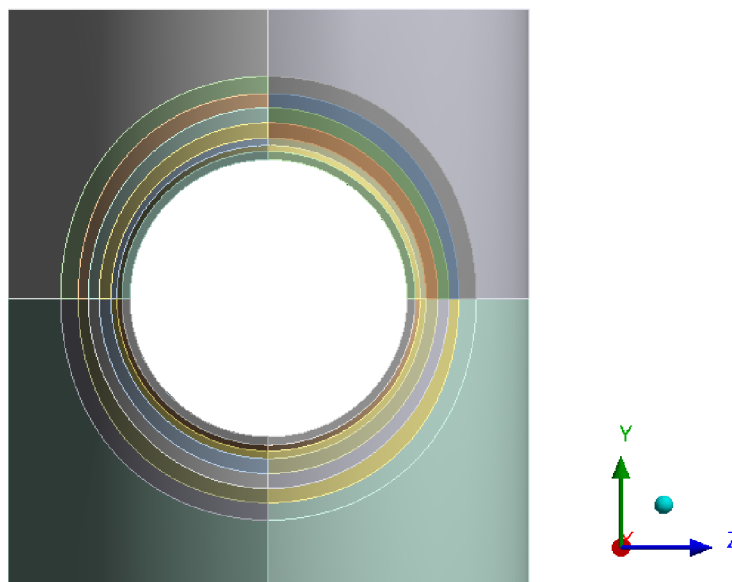


Figure 6.2: FEA model for quadratic extrapolation

# Attachment 3

## Stress intensity of shell and solid models

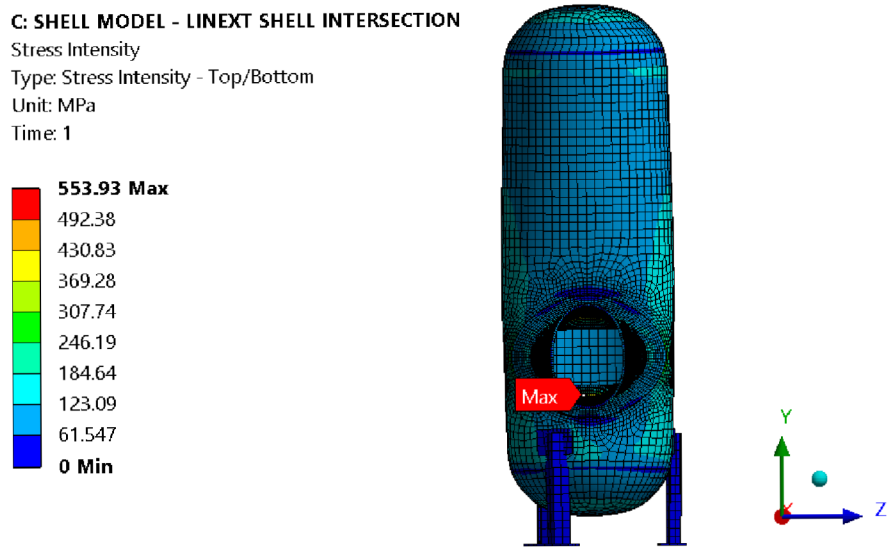


Figure 6.3: Stress intensity of shell-element model

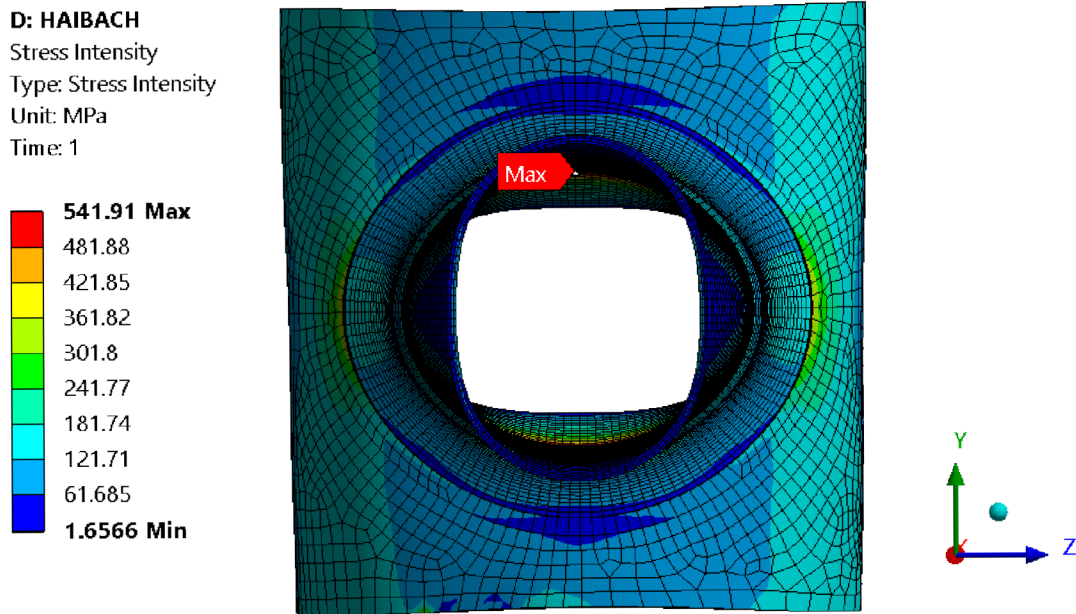


Figure 6.4: Stress intensity of solid-element model

# List of Figures

3.1	Pressure cycles right before the fatigue failure [6] . . . . .	5
3.2	Representation of the four fatigue phases in ductile metals before failure [4] . . . . .	6
3.3	Stress cycle parameters [18] $\sigma_a$ – stress amplitude; $\sigma_m$ – mean stress of the cycle; $\sigma_{max}$ – maximal applied stress; $\sigma_{min}$ – minimal applied stress; $\Delta\sigma$ – stress range . . . . .	7
3.4	S–N curve for unnotched low–alloy steel specimens [7] . . . . .	8
3.5	S–N curves for steel categorized in FAT classes; standard application [2] . . . . .	9
3.6	S–N curves for steel categorized in FAT classes, very high cycles applications [2] . . . . .	10
3.7	Fatigue assessment of welded components – detailed procedure [10] . . . . .	13
3.8	Structural stress determination methods according to Annex NA [8] . . . . .	15
3.9	Representation of deviations from designs shape at the seam welds, taken from [10] . . . . .	15
3.10	Common types of macro–geometric effects where: a) large openings; b) curved beam; c) shear lag; d) flange curling; e) discontinuity stresses in a shell; f) bending due to lap joint eccentricity [2] . . . . .	19
3.11	Local structural discontinuities: (a) gusset plate; (b) variation in width; (c) cover plate end; (d) stiffener end; (e) variation in plate thickness. [15] . . . . .	20
3.12	Local stress distribution in vicinity of a weld toe [15] . . . . .	21
3.13	Increase of a stress cycle amplitude at the weld toe [20] . . . . .	22
3.14	Modes of fatigue failure of a fillet weld [22] . . . . .	22
3.15	Fillet weld parameters [22] . . . . .	23
3.16	Typical weld imperfections [20] . . . . .	23
3.17	Examples of stress improvement methods [20] . . . . .	24
3.18	Examples of weld modelling techniques using shell elements [21] . . . . .	25
3.19	Graphical representation of stress evaluation methods [16] . . . . .	27
3.20	Typical hot–spot stress evaluation paths used for FEA (stress along the edge does not depend on the material thickness, stress along the surface depends on the material thickness) [2] . . . . .	28
3.21	Location of reference points at a shell model with a relatively coarse mesh [12] . . . . .	29
3.22	Linear extrapolation based on two specified reference points [10] . . . . .	30
3.23	Quadratic extrapolation based on three reference points [10] . . . . .	31
3.24	Through–wall linearization across the cross section at the weld toe (hot–spot)[10] . . . . .	31
3.25	Approximation of the fillet weld by a spline according to the CAB–concept [10] . . . . .	32
3.26	Hot–spot stress determination according to the Haibach concept [10] . . . . .	33
3.27	Effective radius of weld toes and roots (left) and a model example of FEA (right) [24] . . . . .	34
4.1	Solidworks model of the simplified vessel geometry . . . . .	35
4.2	Detail of the shell/nozzle junction . . . . .	36
4.3	Diagram of the Ansys project . . . . .	37
4.4	Shell model in Ansys (the individual colours represent thicknesses in mm) . . . . .	38

*LIST OF FIGURES*

4.5	Shell/nozzle junction with reference points and paths for the linear extrapolation . . . . .	39
4.6	Shell/nozzle junction with reference points and paths for the quadratic extrapolation . . . . .	39
4.7	Appropriate mesh for the subsequent analysis of the shell model . . . . .	40
4.8	Boundary conditions of the shell model . . . . .	41
4.9	Force simulating the pressure on the flange . . . . .	41
4.10	Deviation in the distance along the surface between evaluation paths . . . . .	42
4.11	Possibly problematic connection of parts . . . . .	42
4.12	Shell to solid sub-modeling . . . . .	43
4.13	Geometry of sub-models with a triangular weld, here represented by a model according to the Haibach method . . . . .	44
4.14	Geometry according to the CAB-method with a fillet radius . . . . .	44
4.15	Appropriate mesh for the subsequent analysis of the solid submodel . . . . .	45
4.16	Appropriate mesh for the subsequent analysis of the solid submodel . . . . .	46
4.17	The tensile force at the nozzle end of the submodel . . . . .	46
4.18	Section of one of the sub-models in SolidWorks: a) model with overlapping bodies; b) repaired model (partially remodelled) . . . . .	47
4.19	Reference points for the comparison of the stress determination methods . . . . .	48
6.1	FEA model for linear extrapolation . . . . .	60
6.2	FEA model for quadratic extrapolation . . . . .	60
6.3	Stress intensity of shell-element model . . . . .	61
6.4	Stress intensity of solid-element model . . . . .	61

# List of Tables

3.1	Stress evaluation methods for welded structures (table taken entirely from [2]) . . . . .	26
4.1	Technical parameters of the vessel . . . . .	36
4.2	The assigned fatigue class given in Table 18–7 of [10] . . . . .	48
4.3	Shell–element model analysis results . . . . .	49
4.4	Solid–element model analysis results . . . . .	49